The vegetation, climate, and fire history of a mountain steppe: A Holocene reconstruction from the South Caucasus, Shenkani, Armenia

Amy Cromartie, Claire Blanchet, Chéima Barhoumi, Erwan Messager, Odile Peyron, Vincent Ollivier, Pierre Sabatier, David Etienne, Arkady Karakhanyan, Lori Khatchadourian, et al.

Quaternary Science Reviews 246 (2020) 106485

Contents lists available at ScienceDirect

Quaternary Science Reviews

journal homepage: www.elsevier.com/locate/quascirev

The vegetation, climate, and fire history of a mountain steppe: A Holocene reconstruction from the South Caucasus, Shenkani, Armenia

Amy Cromartie [a, *], Claire Blanchet [b], Chéïma Barhoumi [c], Erwan Messager [b], Odile Peyron [c], Vincent Ollivier [d], Pierre Sabatier [b], David Etienne [e], Arkady Karakhanyan [f], Lori Khatchadourian [g], Adam T. Smith [a], Ruben Badalyan [h], Bérengère Perello [i], Ian Lindsay [j], Sébastien Joannin [c]

[a] Department of Anthropology, Cornell University, Ithaca, NY, 14853, USA
[b] EDYTEM, Université Savoie Mont-Blanc, CNRS, Le Bourget du Lac, France
[c] Institut des Sciences de l'Evolution de Montpellier ISEM, Université de Montpellier, CNRS, IRD, EPHE, Montpellier, France
[d] CNRS, Aix Marseille Univ, Minist Culture, LAMPEA, Aix-en-Provence, France
[e] Univ. Savoie Mont Blanc, INRAE, CARRTEL, F-74200, Thonon-les-Bains, France
[f] Institute of Geological Sciences, National Academy of Sciences of Armenia, Yerevan, Armenia
[g] Department of Near Eastern Studies, Cornell University, Ithaca, NY, 14853, USA
[h] Institute of Archaeology and Ethnography, National Academy of Sciences of Armenia, Yerevan 0025, Armenia
[i] CNRS, Archéorient, UMR 5133, Lyon, France
[j] Department of Anthropology, Purdue University, West Lafayette, IN, 47907, USA

ARTICLE INFO

Article history:
Received 19 February 2020
Received in revised form
10 July 2020
Accepted 11 July 2020

Keywords:
Holocene
Paleoclimatology
Southwest Asia
South Caucasus
Vegetation dynamics
Steppe
Fire

ABSTRACT

Steppe and grassland ecosystems constitute important biomes that are influenced by multiple factors such as climate, human activity, and fire. Yet how these factors have influenced the plant composition of these biomes through time continues to be understudied. This paper investigates how these mechanisms have transformed the steppe landscape recorded at the mire site of Shenkani, Armenia. This highland site, located in the South Caucasus, has a long human history of permanent settlements near the core site starting at 5500 cal. BP. A variety of biological and geochemical proxies, including pollen, non-pollen palynomorphs, macro-charcoal, ^{14}C age model, X-ray fluorescence, loss-of-ignition, magnetic susceptibility, and a quantitative climate reconstruction inferred from pollen, are utilized in this paper. We find that this area has remained a steppe with small stands of trees throughout the duration of the Holocene. Changes in steppe plant composition primarily occur between semi-desert steppes (Chenopodiaceae), grassland steppes (or Poaceae dominated meadow-steppes), and mixed steppes with forest patches. In this record, two phases of local grassland expansion occurred between 9500 and 7000 cal. BP and 2500 −1000 cal. BP, which covaried with local fire events. These grassland steppes were sustained until tree encroachment led to a more mixed steppe landscape around 7000 cal. BP and again at 1000 cal. BP. Climate, primarily precipitation, is the main driver of this persistent steppe landscape and the plant compositional shifts within it. However, fire and human activities contributed to steppe maintenance.

1. Introduction

Debates surrounding the origin and persistence of Eurasian steppe biomes throughout the Holocene have historically generated two contrasting hypotheses: (i) the natural formation due to persistent arid climatic conditions (Vysotsky, 1905) after the last glacial maximum (Mulkidzhanian, 1975) (ii) and the formation and modification of steppes by anthropogenic influences (Volodicheva, 2002; Nakhutsrishvili, 2013).

* Corresponding author. 261 McGraw Hall Cornell University Ithaca, 14853, NY, USA.
E-mail addresses: aec277@cornell.edu (A. Cromartie), claire.blanchet@univ-smb.fr (C. Blanchet), cheima.barhoumi@umontpellier.fr (C. Barhoumi), erwan.messager@univ-smb.fr (E. Messager), odile.peyron@umontpellier.fr (O. Peyron), ollivier@mmsh.univ-aix.fr (V. Ollivier), pierre.sabatier@univ-smb.fr (P. Sabatier), david.etienne@univ-smb.fr (D. Etienne), georisk@sci.am (A. Karakhanyan), lk323@cornell.edu (L. Khatchadourian), ats73@cornell.edu (A.T. Smith), berengere.perello@cnrs.fr (B. Perello), ilindsay@purdue.edu (I. Lindsay), sebastien.joannin@umontpellier.fr (S. Joannin).

https://doi.org/10.1016/j.quascirev.2020.106485
0277-3791/

Research investigating the catalysts of transformation among steppe biomes, however, remains limited. In the South Caucasus and highland southwest Asia, paleoenvironmental records often focus on tree expansion (Messager et al., 2013, 2017). However, many areas never become fully forested (Joannin et al., 2014; Leroyer et al., 2016) and instead, climate and anthropogenic impacts on vegetation are seen in compositional changes to steppe plant communities. Today in Armenia, over 50% of the potential vegetation classified by Bohn et al. (2000) is classified as steppe or desert plant communities (calculated from EuroVeg map software, categories M4, M11, B58, B59, P36, N7, O7, O8; Bohn et al., 2000). These biomes stretch from eastern Turkey (Atalay and Efe, 2010) into the Armenian-Javakheti plateau across Armenia, Georgia, Azerbaijan, and Northern Iran (Fig. 1). Rich in floristic diversity, many of these areas are classified as biodiversity hotspots (Connor and Kvavadze, 2008; Akhani et al., 2010; Solomon et al., 2014) and today are home to relic Arcto-Tertiary vegetation (Takhtajan, 1941). In Armenia, steppes and steppe-meadows foster large populations of endemic plant species (Fayvush et al., 2017).

In order to understand steppe biome distribution throughout the South Caucasus, a region marked by contrasting topography and geology, it is necessary to situate existing data within debates over the forces driving landscape change. A persistent question concerns the reasons for a delayed forest expansion in the early and mid- Holocene. Many paleoenvironmental records from the region note the expansion of trees 2000–4000 years after the climate amelioration at the Pleistocene-Holocene transition (ca. 11,700 cal a BP) (Wick et al., 2003; Messager et al., 2013, 2017; Joannin et al., 2014). Multiple hypotheses seek to explain the delay, attributing it to distance from tree refugia (Messager et al., 2013), shifts in seasonal precipitation (Wick et al., 2003; Joannin et al., 2014; Messager et al., 2017), and suppression by both natural and human driven fire events (Roberts, 2002; Turner et al., 2008, 2010). These arguments provide an understanding of the mechanisms operating within forested areas; however, they fail to consider how this phenomenon takes shape in steppe environments.

Human activity is well-documented in records of Holocene landscapes throughout the South Caucasus (Connor, 2011; Messager et al., 2013; Joannin et al., 2014) and greater southwest Asia (Djamali et al., 2009; Roberts et al., 2011; Woodbridge et al., 2019). In the Caucasus, early cereal farming and sheep/goat pastoralism date to the sixth millennium cal. BC (Chataigner et al., 2014). The extent of human influence on landscape vegetation, however, continues to be debated. Many researchers argue that large-scale agriculture and pastoral practices gave rise to the steppe vegetation seen across the region today (e.g. Volodicheva, 2002; Nakhutsrishvili, 2013, also see Connor, 2011 for discussion). Records from Georgia (Connor, 2011) and Armenia (Zarishat: Joannin et al., 2014; Vanevan: Leroyer et al., 2016) have challenged these narratives. They demonstrate the dominance of steppe taxa prior to the introduction of permanent settlements and agricultural practices. To understand the complexities of landscape change, paleoenvironmental studies need to consider and combine multiple factors into new models of landscape formation and maintenance, including climate change, human activities, and fire events. Under the auspices of an intensive coring program in the Kasakh valley of Armenia, we have documented a 10,240-year continuous sediment record from the mire site of Shenkani. Continuous records of this length are rare in the South Caucasus. Utilizing a multi-proxy approach, we aim to investigate how the convergence of fire, climate, and humans have shaped this steppe landscape.

2. Study area

2.1. Geological and climate settings

Located on the Armenian-Javakheti plateau, Shenkani mire (40°37′55.85″ N; 44°16′45.86″ E; 2186 meters above sea level [m a.s.l.] Fig. 1) sits in a volcanic depression on the north-eastern flanks of Mount Aragats (4095 m a.s.l) in the Kasakh valley. This area of northern Armenia boasts some of the largest concentrations of wetlands and peatlands in the country (Jenderedjian, 2005).

The geological environment is a product of Pliocene-Quaternary volcanic activity and the collision of the Arabian and Eurasian continental plates (Chernyshev et al., 2002; Volodicheva, 2002). The Mount Aragats volcanic massif was primarily active between ~1.5–.5 Ma and is composed of tuffs, basaltic, and andesitic lava flows (Mitchell and Westaway, 1999; Chernyshev et al., 2002; Gevorgyan et al., 2020). While it is suggested that eruptions continued into historical periods (Nalivkin, 1973), today, the Aragats' volcano remains inactive. The elevation in this area ranges from 4095 m a.s.l. at the peak of Mount Aragats to 1800 m a.s.l. in the Kasakh river valley (Fig. 2a). At the end of the Upper Pleistocene, the basaltic slopes were occupied by accumulations of permanent snow and dead ice tongues that formed into erosive cells. Several topographical cells, including Shenkani, that today house lakes, were first created from the repetitive melting of glacial features during the post-glacial periods. Due to its volcanic composition, lake catchments are small with only short or non-permanent tributaries; this enabled their development into mires over time.

The Armenian-Javakheti volcanic plateau is characterized by its high level of continentality and sits in the western ranges of the Lesser Caucasus mountains (Volodicheva, 2002). The plateau's inland location, away from the Black and Caspian Seas, as well as its geographic structure (higher around the edges, lower in the middle), allows for high-pressure systems in winter and low-pressure systems in the summer (Lydolph, 1977). This seasonal high-pressure system and radiational cooling facilitate lower than expected temperatures for this latitude (Volodicheva, 2002). On the Armenian-Javakheti plateau, precipitation is highest in May–June, due to the annual advancement of a regional polar front, which transitions to drought-like conditions accompanied by high temperatures beginning in July (Volodicheva, 2002). Precipitation on the plateau is higher in the north and dwindles towards the south. Due to the higher elevation, the Shenkani environs receive more precipitation and have lower temperatures than the plateau's lowland. The compiled meteorological records from the Aparan weather station, located 14 km south of the mire, records an annual average temperature of 4.7 °C and temperatures are highest in July and August (Fig. 1b). Annual precipitation is 703.6 mm, with the highest levels occurring in May and June and the lowest in August and September. Annual precipitation of 586 mm and an annual average temperature of 3.63 °C at the core site is recorded by point analysis in QGIS from interpolated worldclim2 data (Fick and Hijmans, 2017). In the late spring and early summer, short afternoon thundershowers are common, with occasional hail. Snow often accumulates on the high northern mountain peaks of Mount Aragats. During the winter, the snowline descends in elevation, reaching the lowest levels on the Tsaghkahovit plain, while snowmelt feeds spring pastures throughout the summer (Smith et al., 2009). Permanent snowfields are no longer present in Armenia (Nestler et al., 2014). Davoyan (1971) reported mountain glaciers between 1957 and 1965 on Mount Aragats, but noted they had almost completely disappeared by the time of his report.

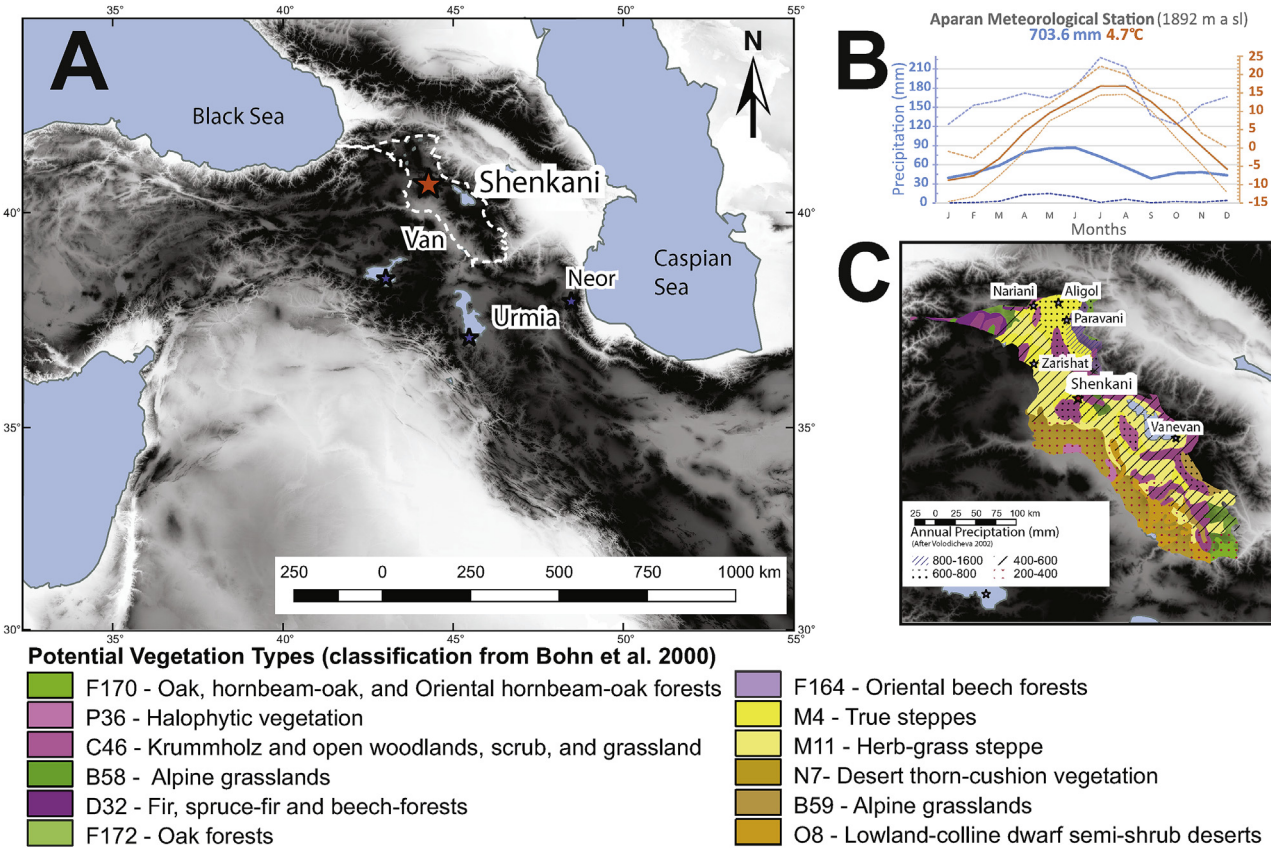

Fig. 1. Maps of part of highland southwest Asia and Caucasus A.) Select sites discussed in the text on the topographic map. The white outline represents the Armenia-Javakheti plateau from Volodicheva (2002). DEM Source: GTOPO30 (Earth Resources Observation and Science Center, 1997; https://doi.org/10.5065/A1Z4-EE71) B.) Ombrothermic diagram from the city of Aparan meteorological station. Data compiled from years: precipitation: 1936–1996 & 1998–2008; temperature:1935–1985 & 1987–2008. C.) Potential vegetation for the Armenia-Javakheti plateau (Bohn et al., 2000) with precipitation map superimposed (Volodicheva, 2002).

2.2. Present day vegetation

The vegetation of Armenia is diverse and follows altitudinal zonation. Semi-desert areas are found in lower mountain belts (480–1200 m a.s.l.) while forest, meadow-steppe, shrub-steppe, and thorny cushion vegetation occur in the middle and upper-mountain belts (1200–2200 m a.s.l.) (Fayvush et al., 2017). Subalpine and alpine belts are rich in meadows and carpet meadows (2200–4000 m a.s.l.) (Fayvush et al., 2017). In the area of the Kasakh valley and Tsaghkahovit plain, Bohn et al. (2000) has defined four potential vegetation classifications (Fig. 2a): (i) steppe and meadow steppes composed primarily of Poaceae, including species of *Festuca, Stipa, Bromus, Elymus, Koeleria* along with wild variations of cereals (*Secale montanum, Hordeum violaceum*); (ii) Trans-Caucasian feather grass steppe, replete with *Stipa*, *Festuca-Stipa*, and herbs in the Tsaghkahovit plain; (iii) sub-alpine vegetation, including mixed-steppe forests comprised of *Quercus macranthera* forest, *Acer trautvetteri*, *Betula litwinowii*, and species of Poaceae, including *Festuca* and *Stipa* on the northeastern side of Mount Aragats and the western side of the Pambak mountain range; (iv) alpine vegetation, including *Kobresia* and *Carex* grasslands and species of *Rhododendron caucasicum, Campanula*, and *Carum caucasicum* on the highest peaks of Mount Aragats (Bohn et al., 2000). Although vegetation maps and onsite surveys were utilized by Bohn et al. (2000), the observed vegetation may differ. Today, this area is mostly devoid of trees, but mixed steppe-oak forests can be found on the western slopes of the Tsaghkunyats and Pambak mountain ranges. Rows of pines, planted during the 1980s, are present in both the Kasakh valley and Tsaghkahovit plain. Dry farming of barley and fodder predominates in the flat areas, while the lower mountain slopes serve as pasture for cattle, sheep, and goats. At lower altitudes, farmers use the bog meadows for haymaking (Jenderedjian, 2005).

The Shenkani mire hosts a variety of water plants, including multiple species of Cyperaceae, including tussocks of *Carex*, which cover most of the mire's surface (Fig. 2b–c). After spring rains, free water accumulates along the shore where livestock is often watered. Trees are absent around the basin. The surrounding grass steppe includes various species of Poaceae, *Artemisia*, and Asteraceae. Additionally, *Campanula* and Ranunculaceae are found growing on the wetland itself. Select parts of the Kasakh valley, Tsaghkunyats, and Pambak mountain range are considered priority conservation sites by the World Wildlife Fund's (WWF) Critical Ecosystem Partnership Fund (Solomon et al., 2014, Fig. 1).

2.3. Archaeological evidence and human settlements

Extensive archaeological exploration has documented the long history of human habitation in the Tsaghkahovit plain and Kasakh valley, with the earliest evidence dating to the Lower Paleolithic (Gasparyan et al., 2014). During the Holocene, the first signs of human occupation are Mesolithic hunting sites that were occupied for short periods in the lower Kasakh valley (Arimura et al., 2012). While there is some evidence of Neolithic occupations on the Tsaghkahovit plain (Smith et al., 2009; Arimura et al., 2012) and Chalcolithic occupations in the lower Kasakh valley (Arimura et al.,

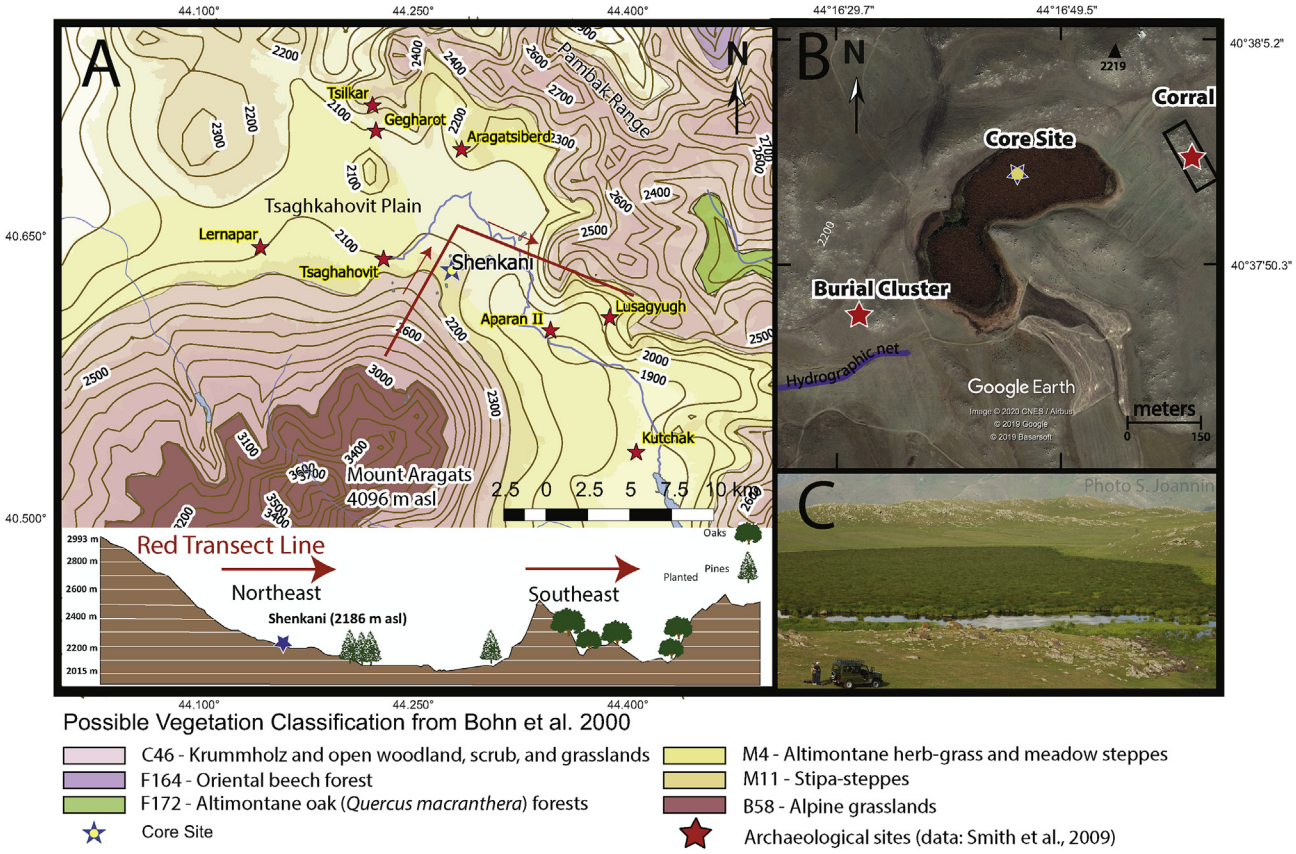

Fig. 2. Local maps of the Kasakh valley and Tsaghkahovit plain A.) Elevation map of the Kasakh valley and Aragats volcano with potential vegetation classifications. The red line is a simulation/recreation of aboreal vegetation transect seen below based on data from Google Earth. Data sources: elevation information Aster DEM (ASTER GDEM is a product of METI and NASA), archaeology sites (Smith et al., 2009), potential vegetation, (Bohn et al., 2000), elevation profile (modified from Google Earth). B.) Image modified from Google Earth (Image © 2020 CNES/Airbus, © 2019 Google, © 2019 Basarsoft) of the Shenkani wetland with associated archaeology sites. C.) View of the southern sub-basin of Shenkani covered by Cyperaceae tussocks. (For interpretation of the references to colour in this figure legend, the reader is referred to the Web version of this article.)

2012) overall evidence from these periods remains limited (Smith et al., 2009).

The first permanent sites in the region date to the initial centuries of the Early Bronze Age (ca. 3500–2400 BC); however, during the Middle Bronze Age (ca. 2400–1500 BC), a wide-scale shift to mobile lifeways reshaped communities across the South Caucasus (Smith, 2015). Archaeological evidence of human occupation in the Kasakh valley during this period primarily comes from mortuary sites (e.g., Verin Naver) and occasional ephemeral traces at settlement sites (e.g., Aparani Berd). Large-scale permanent settlement returned to the region ca. 1500 BC, with significant occupations during the Late Bronze Age (ca. 1500–1150 BC), Iron 1 (ca. 1150–800 BC), Iron 2 (ca. 800–600 BC), and Iron 3 (Achaemenid, ca. 600–300 BC) periods (Manning et al., 2018). Subsequently, archaeological and epigraphic sources suggest human activity in antiquity, the Medieval period, and into the modern era (Smith et al., 2009).

The settlement history of this region has and remains the focus of extensive excavations and surveys by the joint American-Armenian Project for the Archaeology and Geography of Ancient Transcaucasian Societies (a.k.a., Project ArAGATS) (Badalyan et al., 2008, 2014; Khatchadourian, 2014; Smith et al., 2009; Smith, 2015). Project ArAGATS's investigations recorded hundreds of archaeological sites, including burial clusters, settlements, fortresses, dating from the Neolithic to the present day (Smith et al., 2009). Excavations from the Early Bronze to the Medieval periods have unearthed settlement and mortuary contexts at sites such as Gegharot (Smith and Leon, 2014), Tsaghkahovit (Lindsay, 2006; Khatchadourian, 2008, 2014; Marshall, 2014), Aparani Berd (Badalyan and Avetisyan, 2007), Arai (Franklin, 2014a), and Aragatsi Berd (Greene, 2013). Extensive archaeobotanical and zooarchaeological analyses from these operations revealed a mixed agro-pastoral economy during the Bronze and Iron Age, focused on cereal agriculture and domesticated animals such as sheep, goat, cattle and in some instance horses and pig (Hovsepyan, 2008, 2014; Monahan, 2008, 2014; Badalyan et al., 2014).

3. Methods

In 2012, two 356-cm parallel-cores were recovered from Shenkani mire. The shape of the basin, divided into two sub-basins, allowed us to drill into the sub-basin located further from the basin's edge (Fig. 2b). Here, the sediment is less impacted by discharge, including flood events, and thus is more resilient to drying. Utilizing a Russian corer with a 5 cm diameter chamber, our team retrieved two parallel cores in 11 sections. At the EDYTEM laboratory, each half-section was described in detail and recorded photographically. Drafting lithological descriptions of the sequence allowed for the identification of different sedimentary facies. A complete master core (MC) was created by combining the lithological sequence and X-Ray Fluorescence (XRF) core scanning from both parallel cores. This resulted in the production of a single 356 cm long core profile.

3.1. Geochemical and sedimentology analyses

The down-core chemical composition analysis of each core section was performed using an Avaatech XRF (EDYTEM Laboratory) core scanner at 5 mm intervals across the split core surface. The split-core surface was first covered with 4-mm-thick Ultralene foil. Geochemical data were then obtained with two tube settings. For Si, Mn, K, Ti, Al, S, Fe, Ca elements, analysis was conducted at 10 kV at 10 s; for heavier elements, Sr, Rb, Zr, Br, and Pb analysis was conducted at 30 kV at 30 s (Richter et al., 2006). Each power spectrum was converted into relative components (intensities) expressed in counts per second. Due to the influences of variable water content and grain size in the sediment matrices, the XRF scanner provides an estimate of the geochemical composition, and the acquired counts are semi-quantitative (Croudace and Rothwell, 2015). In order to understand organic production and terrigenous inputs, a bromine titanium ratio (Br/Ti) was created. Titanium (Ti) records terrigenous inputs that are less impacted by weathering and redox processes (Arnaud et al., 2012) and bromine (Br) can indicate organic matter (Bajard et al., 2016).

To obtain geophysical measurements the core sections were subsequently logged with a GEOTEK Multi-Sensor Core Logger [gamma-ray wet bulk density, magnetic susceptibility (MS), p-wave velocity] at 5 mm intervals. Loss on Ignition (LOI) analysis was carried out to estimate the organic content of the sediment, following the procedure by Heiri et al. (2001). In total 104 samples were collected at 1–4 cm intervals and dried. Dried samples were weighed prior to and after each heating. For organic matter estimates, samples were placed in an oven with an ignition of 550 °C for 5 h.

3.2. Radiocarbon dating

Chronological information was obtained through ^{14}C dating on plant macrofossils processed by accelerator mass spectrometry (AMS) at the Poznan and Gif sur Yvette laboratories (Table 1). Samples were processed with an acid, base, acid pre-treatment prior to dating. Materials used for dating included seeds, peat macro-remains, and plant fibers. Collected samples were sieved using a 100 μm mesh screen and organic matter was separated under a stereo microscope. Radiocarbon ages were calibrated in cal. BP using the IntCal13 calibration curve (Reimer et al., 2013). Dates are expressed as intercepts with a 2σ range. The age-depth model was constructed using a smooth spline (Fig. 3b) with the R 'Clam' package developed by Blaauw (2010).

3.3. Pollen analysis

Pollen samples were extracted across the core at 1–3 cm resolution and treated with standard procedures (Moore et al., 1991; Faegri and Iversen, 1989) including acetolysis, sieving, and chemical treatment of 10% mixtures of HCl and KOH. HF was utilized as a subsequent treatment if necessary. In total 87, samples were analyzed (28 as part of Blanchet, 2017) and 8 were marked sterile due to low pollen concentrations. A higher resolution record was analyzed in sections B2-A5, during periods of human occupation, to provide a better understanding of the influence of climate on human societies. Cereal grains and the coprophilous fungus *Sporormiella* were counted to assess potential periods of human impact. Pollen was analyzed by light microscopy at a standard magnification of 400×. Each slide was counted with a goal of 300 terrestrial pollen grains, excluding aquatic plants (i.e. Cyperaceae and *Nymphaea*) and spores. Pollen atlases (Reille, 1992–1998; Beug, 2004) and the reference collection at the Institut des Sciences de l'Evolution at the University of Montpellier were utilized to aid in identification. In total, 67 unique taxa were identified. Aquatic vegetation, fungal spores, algae, and non-pollen polymorphs (NPP) were counted alongside pollen taxa to a terrestrial pollen count of 300. Due to the abundance of certain aquatic taxa (Cyperaceae/*Botryococcus*), aquatic and NPP percentages were calculated separately from terrestrial pollen in order to isolate the local lake ecology from the landscape signal. Based on results from pollen PCA analysis, ratios of steppe taxa were calculated by dividing (Poaceae +1)/(Chenopodiaceae +1) to understand changes from a semi-desert steppe to grassland. A ratio for *Artemisia* and Chenopodiaceae (*Artemisia* + 1)/(Chenopodiaceae +1) was also created due to the possible association of some Poaceae species with the wetland. This ratio separates the desert from steppe plants (El-Moslimany, 1990).

3.4. Macro-charcoal

Macro-charcoal was sampled at a volume of 0.5 cm^3 and 1 cm^3 at contiguous 1 cm intervals across the master core. Samples were soaked for a minimum of 2 days in a solution of sodium metaphosphate (3 g), potassium hydroxide (0.5g), and 30 ml of bleach. Each sample was wet sieved through a 160-μm diameter sieve to isolate particles related to local fires. In open landscapes, this mesh size is associated with fires <5 km from the source area (Aleman et al., 2013; Leys et al., 2015). This differs from forested landscapes where this mesh size is primarily associated with a distance <1 km (Higuera et al., 2007). We utilized a 20× stereo microscope to identify charcoal particles and image-analysis software (WinSEEDLE™, Regent Instruments Inc.) to measure the width, length, and area of each charcoal. We then utilized CharAnalysis (Higuera et al., 2009; available for download from http://charanalysis.googlepages.com) for statistical analyses. On both $Char_{area}$ and $Char_{count,}$ we resampled the char series to a constant time resolution of 32 years ($C_{interpolated}$). In order to identify significant peaks, we deployed a 1000-year loess smoothing window that is robust to outliers with a local configuration and a signal to noise index >3 (Kelly et al., 2011) on $Char_{area}$ measurements. To separate noise (caused by sediment mixing and/or issues with statistical analysis) from peaks, we applied a Gaussian mixture model with a threshold in the 99th percentile, dividing $C_{background}$ and C_{noise}. Next, $C_{background}$ was subtracted from $C_{interpolated}$ to obtain C_{peak} values. $Char_{accum}$ is $C_{interpolated}$ calculated to count (#/cm^{-2}/yr^{-1}; $Char_{count}$) or area (mm^{-2}/cm^{-2}/yr^{-1}; $Char_{area}$). For width and length analysis, we utilized W/L ratio calculations from measurements recorded with WinSEEDLE™. We utilized the W/L measurement for each charcoal particle and then calculated the mean and median of each sample to provide information about fuel type (Aleman et al., 2013).

Partial Redundancy Analysis (RDA) was performed with library vegan (Oksanen et al., 2019) to establish the relationship between human impact, fire, and vegetation. To do this, the area $Char_{accum}$ record and pollen record were resampled to a constant time series of 130 years (mean of pollen record) with linear interpolation. Pollen taxa with at least 1 sample that was >5% of the total assemblage were chosen for analysis. Since percentage data are not normally distributed, pollen data was first transformed with a square-root transformation (Legendre and Birks, 2012). Human occupation periods were established by presence and absence based on the chronological model in Manning et al. (2018). Periods with known archaeological stratigraphic sequences were assigned a 1, while periods of abandonment, were given a 0. For the last 2000 years, we assigned a 1 since there has been some evidence of human presence in the area since the antique period (Smith et al., 2009), and the resolution of our record during this time does not allow us to break down each period further. A partial RDA was run

Table 1
AMS-radiocarbon dates from Shenkani with a 2σ range of calibration utilizing an IntCal 13.14C calibration. Age A2 52_53 was rejected for being out of sequence with a carbon content of 0.3 mg C.

Depth MC (cm)	Sample ID	Lab. code	Material	AMS 14C (age BP)	Cal yr BP (2 σ)
31.5	A1 54-55	Gif 43880	Peat macro-remains	55 ± 30	0–256
63	B1 54-55	Poz-76409	Plant fibers	185 ± 30	0–299
81	A2 36_37	Gif 48875	Plant fibers	1140 ± 30	969–1168
97	A2 52–53*	Poz-76411	Plant fibers	825 ± 35	679–792
99	B2 18-19	Poz-86017	Plant fibers	2390 ± 35	2342–2681
101	B2 20-21	Poz-86018	Plant fibers	2345 ± 35	2215–2485
135	B2 54-55	Gif 43879	Peat macro-remains	3580 ± 60	3702–4077
170	A3 53-55	Gif 43883	Peat macro-remains	4530 ± 70	4965–5448
204	B3 51-52	Poz-76412	Plant fibers and seeds	5670 ± 40	6322–6558
231	A4 42-43	Gif 43882	Seeds	6450 ± 35	7293–7429
274	B4 49-50	Poz-76413	Seeds	7540 ± 50	8206–8421
313.5	A5 52-54	Gif 43881	Seeds and peat	7970 ± 45	8649–8895
356	A6 55-56	Poz-52956	Plant Fibers	9100 ± 50	10190–10401
	* Rejected Age				

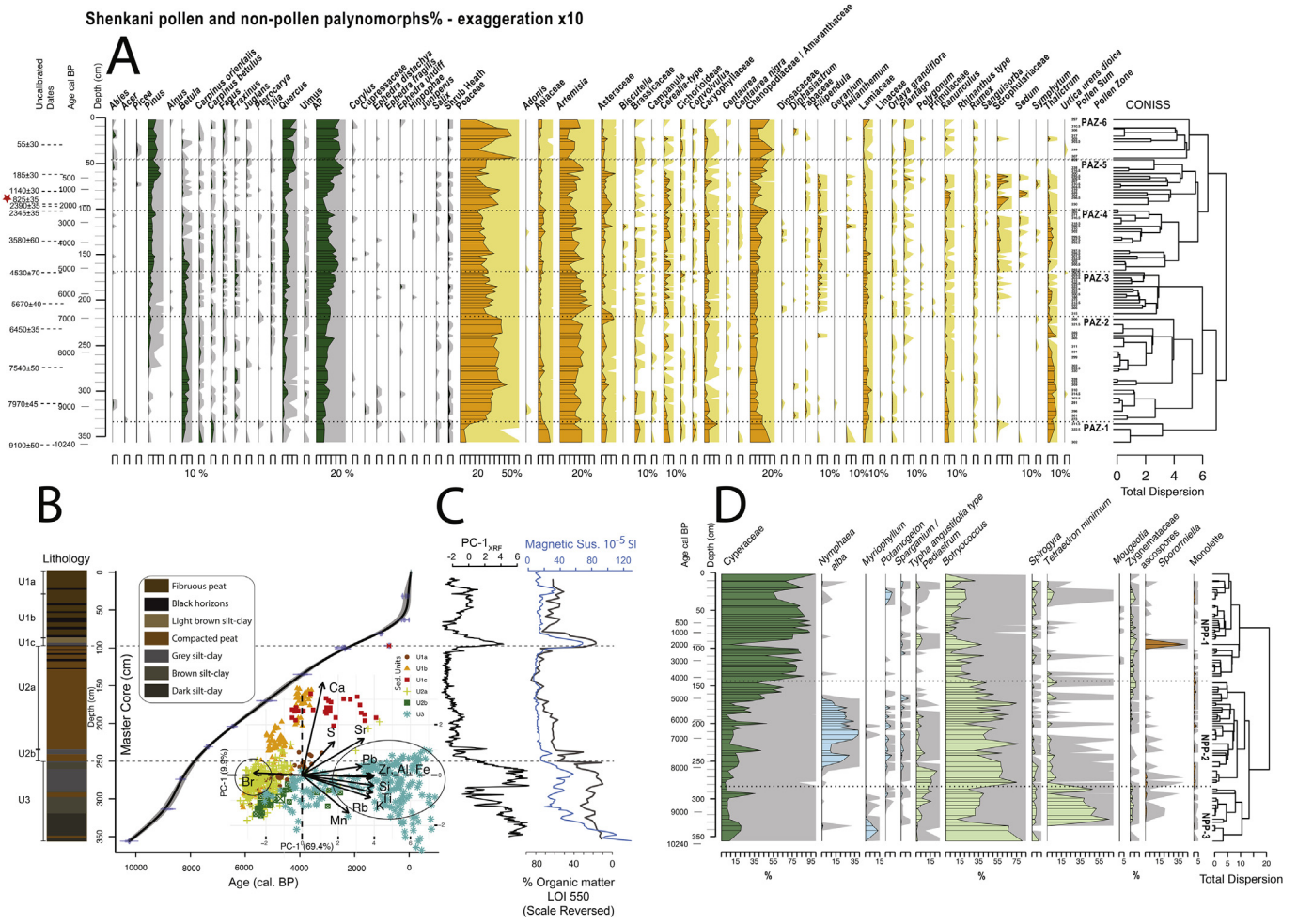

Fig. 3. Pollen and sedimentology arranged by depth A.) Select pollen taxa percentages arranged by depth. Taxa in green represent arboreal and shrub/heath taxa while yellow represents herbaceous pollen. PAZ represents pollen zones by CONISS divisions. B.) The sediment lithology of Shenkani's core is numbered as units (1–3) next to an age-depth model based on calibrated radiocarbon ages (with 2σ errors) (AMS, see Table 1); Principal Component Analysis (PCA_{xrf}) of core scanner measurements on main elements (see 4.1). Circles represent organic and terrigenous endmembers. C.) PC-1 of PCA_{xrf} elements (i.e., Ca, Sr, S, Pb, Zr, Fe, Ti, Al, Si, K, Rb, Mn, Br), magnetic susceptibility, and loss-on-ignition 550 values plotted by depth. D.) Select aquatic pollen and non-pollen palynomorphs including Cyperaceae (in dark green), aquatic and semi-aquatic plants (light blue), algae (light green), and spores (brown) plotted by depth with NPP zones by CONISS divisions. (For interpretation of the references to colour in this figure legend, the reader is referred to the Web version of this article.)

for pollen, human occupations, and $Char_{accum}$, with a condition of age to control for the variation based on chronological autocorrelation (Colombaroli et al., 2009).

3.5. Pollen-based quantitative climate reconstruction

Precipitation reconstructions across the Holocene were

conducted utilizing the Modern Analog Technique 'MAT' (Guiot, 1990). This method was previously tested on samples from Zarishat, Armenia (Joannin et al., 2014) and Vanevan Peat (Leroyer et al., 2016). MAT is not a transfer function but an assemblage approach. With this technique, fossil pollen samples are compared with modern pollen surface samples in terms of taxa composition and abundance. The similarity between each fossil sample and modern pollen assemblage is evaluated by a squared chord distance. Once a set of modern samples has been selected as analogs (modern samples that have the smallest distance), climatic parameters are assigned to each fossil sample as the weighted average of the climate parameters of the modern samples that are the best analogs. The number of analogs chosen in this study was four, using a leave-one-out cross-validation test.

Following Peyron et al. (1998), we applied a biome constraint during analog selection to reduce uncertainties in our climate reconstruction. This enabled us to better distinguish between warm and cold steppes (Tarasov et al., 1998), which is important in our record. To synthesize, a biome is assigned to each modern and fossil pollen assemblages, using the method of Prentice et al. (1996), and Peyron et al. (1998), in which the biome assigned to the selected modern analog is then compared to the biome assigned to the fossil assemblage. Only the analogs with consistent biomes (here cold steppes) are retained for the matching step. To improve our matches, we added 76 new pollen samples from the Southern Caucasus (Armenia) and Mongolia to our dataset (Robles M. pers. comm.; Dugerdil et al., 2020 in review). At Shenkani, we utilized 78 pollen core samples in conjunction with more than 3000 modern pollen samples. Cyperaceae percentages were excluded here because these taxa are considered to be aquatic and their inclusion may result in a biased reconstruction. We reconstructed annual and summer precipitation at Shenkani.

3.6. Statistical and geographic analysis

All statistical analyses, except for CharAnalysis, were undertaken with statistical program R (version 3.4.3; R Development Core Team, 2017). Stratigraphic diagrams of pollen, NPP, charcoal accumulation rates, along with the CONISS functions, were created with package rioja (Juggins, 2017). Additional packages ade4 (Dray, 2007) and factoextra (Kassambara and Mundt, 2017) were utilized for principal component analysis (PCA). RDA analysis was undertaken with package vegan (Oksanen et al., 2019). All maps for figures were created in Quantum GIS (Quantum, G. I. S. Development Team, 2016).

4. Results

4.1. Sediment lithology and composition

Lithological descriptions divided the core into three units from its top to base (Fig. 3b). Unit 1 (0–99 cm) is composed of fibrous peat (gyttja) sediment which starts with silt-clay on a black horizon (Unit 1c) and transitions from dense (Unit 1b) to a less compact accumulation of fibers (Unit 1a). Black horizons, less than a centimeter, are embedded in Unit 1 (grouped for easy representation in Fig. 3b). Compact peat dominates unit 2 (99–252 cm), with grey silt-clay present in Unit 2b and embedded black horizons in 2a. Unit 3 (252–356 cm), is composed of a silt-clay sediment that is black near the bottom and transitions to grey as you move to the top. This unit also contains two layers of compacted peat.

Principal component analysis (PCA) was undertaken on select XRF elements (Sabatier et al., 2010). This isolated two geochemical endmembers: terrigenous (Pb, Zr, Al, Fe, Si, Ti, K, and Rb), and organic (Br) (Sabatier et al., 2010). Major divisions between terrigenous (positive) and organic (negative) loadings occur across principal component-1 (PC-1) which accounts for 69.4% of variability. Br is typically associated with organic matter (Bajard et al., 2016) and a linear regression test revealed a positive relationship between LOI 550 organic matter (OM) and Br (R^2 = 0.57, p-value < 0.001). Therefore, we associate Br with OM. Our results show two periods of increased organic end members in Unit 2a (252 - 99 cm) and in Unit1b-1a (75–0 cm). Three significant increases in terrigenous endmembers are observed, occurring in U3 (356–310 cm & 290–260 cm) and another sudden increase also occurs in U1c (105 - 87 cm). In addition, increases of Mn are recorded in U3 during periods of terrigenous inputs. Magnetic susceptibility (MS) follows a similar trend as Ti and other XRF terrigenous endmembers.

4.2. Chronology

The age-depth model is based on 13 radiocarbon dates (Table 1, Fig. 3b). One determination (Poz-76411; 825 ± 35) was excluded because it was out of sequence and had a low concentration of carbon. The Shenkani record extends from approx. 10240 cal. BP to the present. The average temporal resolution for pollen analysis is estimated to be 130 years. The average sedimentation rate is .75/mm a year (Fig. 6).

4.3. Pollen and non-pollen palynomorphs

4.3.1. Pollen assemblage zones (PAZ)(Fig. 3a)

PAZ-1 (10239–9565 cal. BP; depth 356–336): The beginning of Shenkani's record and PAZ-1 is classified by open semi-arid steppe vegetation, including high levels of Chenopodiaceae (<25%), Caryophyllaceae (<15%), and Apiaceae. These taxa experience a stable decline through this zone. *Artemisia* is present in large quantities, but with little change, while *Thalictrum* and Lamiaceae are found at levels below 10%, but increase slightly. Tree taxa are poorly represented, but small mixes of thermophilous and mesophilic taxa, such as *Carpinus betulus, Carpinus orientalis, Quercus,* and *Betula,* are present in small percentages (<5%). *Carpinus betulus,* and *Carpinus orientalis* decline near the end of this zone, while *Betula* increases.

PAZ-2 (9565–7077 cal. BP; depth 336–222): In PAZ-2 Poaceae, experiences a rapid increase, which indicates the expansion of grasslands. This establishes it as the dominant taxon for the rest of the sequence. Xeric semi-desert steppe taxa, including Chenopodiaceae, and Caryophyllaceae, experience a decline at the expense of Poaceae's increase. Trees and arboreal richness develop, but overall arboreal pollen (AP) levels remain primarly between 10% and 15%. Expansion begins with *Betula* and *Quercus* followed by *Ulmus*, *Fagus*, and *Tilia*. *Pinus* is the last to develop, between 8300 and 7200 cal. BP.

PAZ-3 (7077–5248 cal. BP; depth 222–171): AP continues to develop and increase as taxa become firmly established. Poaceae has a steady decline but remains between 25% and 40%. *Artemisia* increases early in this zone, but steadily declines after its initial increase. Herbs become richer, with increases in Caryophyllaceae, *Cerealia*-type, and *Filipendula*.

PAZ-4 (5248–2411 cal. BP; depth 171–102): After reaching its maximum for the early and mid-Holocene, AP declines (<25%), first with *Betula* at 4700 cal. BP, which never fully recovers, followed by *Pinus* at 4400 cal. BP and *Quercus*. Overall, arboreal taxa richness remains high even with this general decline. Expansions of *Carpinus betulus, Carpinus orientalis, Fagus, Fraxinus, Juglans*, *Pterocarya*, and *Tilia* are seen in this zone. Poaceae also continues its decline along with *Artemisia*. In contrast, Chenopodiaceae steadily rises with a jump around 3800 cal. BP. *Thalictrum*, Scrophulariaceae, and *Rumex* have small increases while other herbs remain stable. At the end of

this zone, there is a slight increase in *Pinus* and *Quercus*, which quickly declines after 3000 cal. BP.

PAZ-5 (2411–93 cal. BP; depth 102–47): The beginning of PAZ-5 shows a sharp increase of Poaceae and other herb taxa, including Scrophulariaceae, *Thalictrum*, and *Ranunculus.* This occurs at the expense of AP, with drops in *Quercus* and *Pinus*. AP increases again in the middle of this zone, beginning with *Pinus*, followed by *Quercus*, which then experiences a subsequent decline and subsequent increase. During this last increase, AP reaches its maximum for the entire record (<30%). With the expansion of AP, Poaceae again regresses, and *Artemisia* becomes the primary steppe taxa. Poaceae rebounds and expands again at the end of this zone.

PAZ-6 (93 cal. BP – present; depth 47–0): PAZ-6 contains the last 93 years of vegetation. At the beginning of this zone, there are expansions in Poaceae, Chenopodiaceae, and *Artemisia,* which decline and then rebound. Poaceae (approx. 30%) and Chenopodiaceae (approx. 20%) reach their maxima. Near the end of this zone, Poaceae again declines and is replaced by *Artemisia* and Chenopodiaceae. Over the last 85 years, *Quercus* and *Pinus* and total AP have remained steady, although there have been small fluctuations in other arboreal species. Other tree taxa are present in small quantities (<2%), including *Abies*, *Picea*, *Betula*, *Carpinus betulus*, *Carpinus orientalis*, *Fagus*, and *Ulmus*.

4.3.2. Aquatics and non-pollen palynomorphs (Fig. 3d)

NPP-1 (10239–8521 cal. BP; depth 356–288): Succession in this zone begins with *Botryococcus*, followed by *Pediastrum*, and Zygnemataceae (ascospores, *Spirogyra*), and *Tetraedron minimum*. The appearance of these algae is indicative of an open water body. Sedges, aquatic, and semi-aquatic plants, Cyperaceae, *Myriophyllum,* and *Typha* are present in small quantities.

NPP-2 (8521–4369 cal. BP; depth 288–147): Algae *Tetraedron* and *Pediastrum* decline at the beginning of this zone, but continue to be present in small quantities. Aquatic and semi-aquatic plants, *Nymphaea alba*, *Sparganium/Typha angustifolia* type, and *Potamogeton* become fully established around 8000 cal. BP as algae declines. Although species fluctuations occur during this period, indicators point to an open lake.

NPP-3 (4369 cal. BP – Present; depth 147–0): Cyperaceae increases during this period, while algae and aquatic plants decline, suggesting a transformation into a wetland. At approximately 2000 cal. BP, there is a significant drop in Cyperaceae and increases in the fungal spore *Sporormiella*, followed by an increase in the algae *Pediastrum* characterizing the possible opening of the wetland. After this, Cyperaceae increases to its maximum in the record then begins a steady decline.

4.3.3. PCA analysis (Fig. 4)

Principal Component Analysis (PCA) was completed on select terrestrial pollen ($PCA_{terrestrialpollen}$) and all aquatic pollen ($PCA_{aquatic}$). For terrestrial pollen, taxa were selected that had at least one sample with a minimum >2% contribution to the total species percentages. PC-1 represents 14.5% of all variance and PC-2, 10.6%. Major divisions across PC-1 occur in arboreal taxa. These correlate with vegetation changes from the early to late Holocene. On one pole, *Betula* has greater positive values and is associated with samples from the early and mid-Holocene, and on the opposite pole, *Quercus* and *Pinus* are associated with the mid- and late Holocene. Across PC-2, a greater variance is reflected in steppe taxa. Here, higher negative values are associated with Poaceae and positive values are associated with herbs such as Apiaceae, Caryophyllaceae, and Chenopodiaceae.

For aquatic pollen, PC-1 represents 27.5% of all variation, while PC-2 represents 20.2%. Division across PC-1 occurs between positive values of Cyperaceae, *Nymphaea alba*, and *Mougeotia*, while negative values are associated with algae species of Zygnemataceae (ascospores, *Spirogyra*), *Tetraedron minimum*, *Pediastrum*, and *Botryococcus*. Aquatic plants *Potamogeton* and *Myriophyllum* are also on this dimension but their contribution is < 5. Across PC-2, positive values are associated with Cyperaceae, *Mougeotia*, Zygnemataceae, *Tetraedron minimum*, *Myriophyllum*, and *Spirogyra*, while negative values are associated with *Pedisatrum, Botryococcus, Potamogeton, Sparganium/Typha angustifolia*-type, and *Nymphaea alba*.

4.4. Macroscopic charcoal analysis

Macroscopic charcoal particles were found throughout the core, providing a fire-history for the duration of the sequence (Fig. 5). Overall, 41 fire peaks were detected. 10 peaks were detected in the early Holocene, 20 in the mid-Holocene, and 11 in the late Holocene. Interpolated $Char_{area}$ and $Char_{count}$ accumulation rates ($Char_{accum}$) show increases between 9150 cal. BP and 4200 cal. BP, after which they then drop off until 2300 cal. BP. That said, there are a few fire peaks between 3740 and 3170 cal. BP. Charcoal accumulation picks up again at 2100–1000 cal. BP. Following this, there is evidence of another hiatus, until the last significant fire event, which occurs during the last 100 years. The mean width to length ratio of all charcoal particles is 0.314 and the mean of the sample mean is 0.277 (Fig. 5), which is consistent with regional open landscape fire histories (see Joannin et al., 2014; Leroyer et al., 2016). Aleman et al. (2013) suggest that charcoal particles with a width/length ratio < 0.5 should be attributed primarily to non-ligneous materials and an open landscape.

Results from RDA analysis examining the relationship with $Char_{accum}$, human occupation periods, and pollen shows a positive correlation with $Char_{accum}$, Poaceae, and Lamiaceae, while a negative correlation occurs between $Char_{accum}$ and other steppe vegetation, including Chenopodiaceae across RDA-1. Across RDA-2, a positive correlation occurs between human occupational periods and Cereals and Asteraceae, while a negative correlation is established between arboreal taxa (*Pinus, Quercus*).

4.5. Pollen based climate reconstruction

For the Shenkani climate reconstruction, analogs were selected from sites located in Armenia, Georgia, and occasionally Kazakhstan, Kyrgyzstan, and Mongolia. For this sequence, all samples fell below the 67.6 threshold (mean random distance = 113.57, standard dev. of random distance = 45.76). The chord distance was also low for our reconstruction (mean distance for the first analog 26.211, mean distance for the last analog 32.526). Results show an average annual precipitation (PANN) of 480 mm, and 144 mm for summer (P_{summer}). The early Holocene is characterized by low precipitation (PANN = 450 mm, P_{summer} 146 mm) which slightly increases in the mid-Holocene (PANN = 487 mm, and P_{summer} = 144 mm), but stays at a similar level during the late Holocene (PANN = 488 mm, and P_{summer} = 143 mm). A major change in precipitation occurs at 9500 cal. BP (10240–9500 cal. BP, PANN = 213 mm, and P_{summer} = 122 mm, 9500–0 cal. BP, PANN = 490 mm, and P_{summer} = 145 mm). The sample near the core top records similar annual precipitation (PANN = 537 mm) to today's worldclim2 value (PANN = 586 mm) from the core site (Fick and Hijmans, 2017).

5. Discussion

5.1. Holocene overview

The sediment record from Shenkani is continuous from

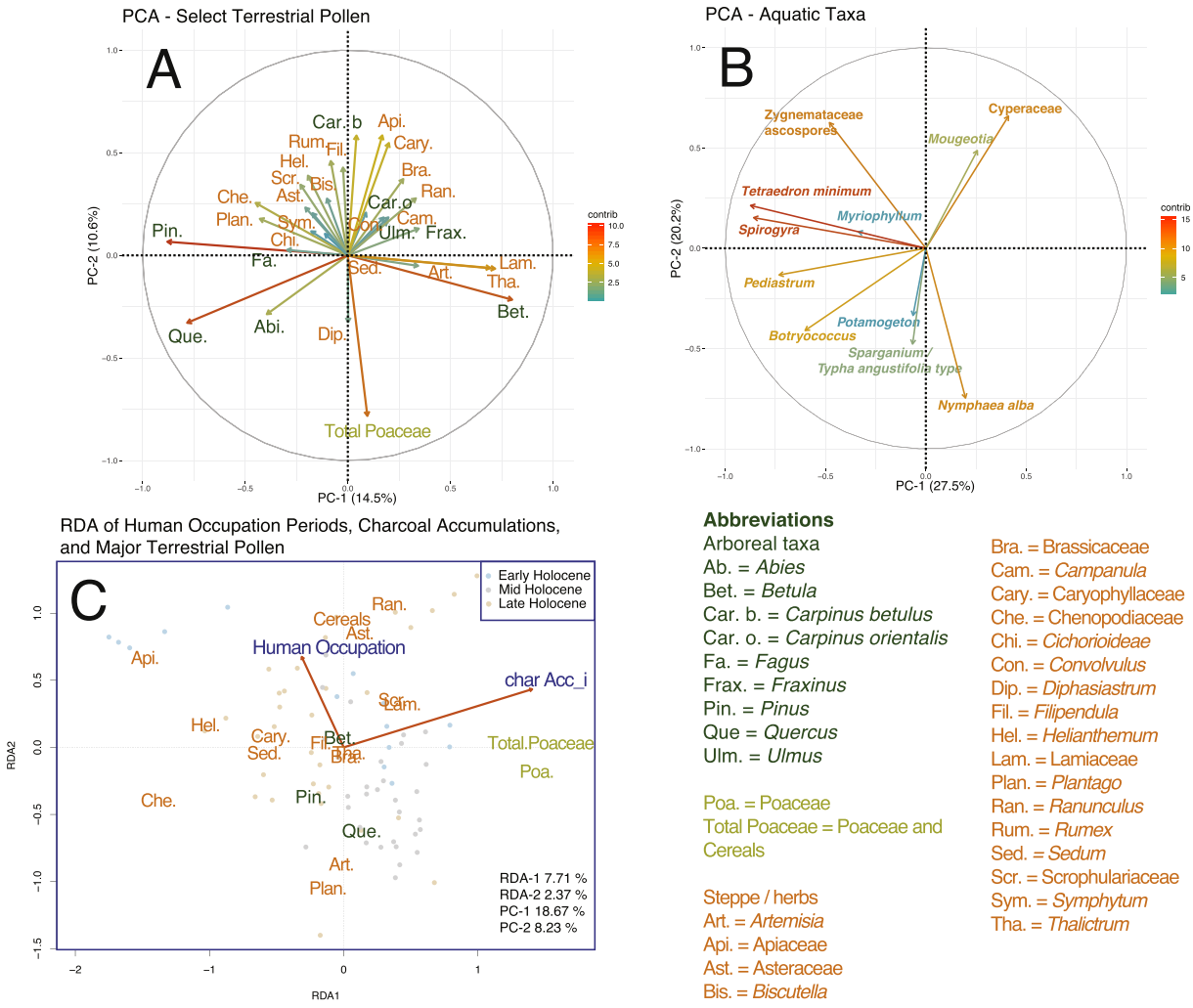

Fig. 4. PCA and RDA analysis A.) PCA bi-plot of select terrestrial pollen ($PCA_{terrestrialpollen}$) taxa (methods: section 3.3) from the Holocene. B.) PCA bi-plot of aquatic pollen ($PCA_{aquatic}$) including algae. C.) RDA bi-plot of select pollen with explanatory variables charcoal accumulation by area and archaeological human occupation periods based on Manning et al. (2018) (section 3.4).

10,240 cal. BP through the present. The terrestrial pollen results show a shifting steppe landscape, with limited forest cover. Throughout the sequence, high values of herb pollen (average NAP > 70%, Fig. 5) record an open landscape dominated by Poaceae, Chenopodiaceae, *Artemisia*, and other herbaceous taxa. This description is similar to the present ecology. The low amounts of arboreal pollen and a mean length to width ratio of 0.314 (mean of all charcoal particles, mean of the sample mean is 0.277) in the charcoal record suggest that the Kasakh valley remained a steppe throughout the Holocene. Rich, but poorly represented trees, suggest distant pollen sources. Sediment attesting to the modern grassland vegetation contains low pollen percentages of *Quercus macranthera*, and *Pinus*, both of which grow today in patches on the slopes of the Kasakh valley (see transect in Fig. 2a), and high percentages of Poaceae, *Artemisia*, and Chenopodiaceae. Pollen grains from *Abies*, *Picea*, and *Pterocarya* also suggest distant pollen transport, since they are not present in Armenia today but can be found in Georgia.

The pollen results also record local non-terrestrial taxa associated with the wetland. The steady curve of $PC\text{-}1_{aquatic}$ (Fig. 5) suggests a stable wetland since the early-mid Holocene transition, which is in agreement with high OM recorded both by $PC\text{-}1_{XRF}$ (Fig. 5) and measured LOI (Fig. 3). After this point, terrigenous elements, eroded from the catchment, are less expressed at the coring point. This is accentuated when the mire is colonized by the Cyperaceae tussocks.

RDA analysis has revealed a relationship between fire and Poaceae biomass. Charcoal accumulation can provide important information about biomass burning (Carcaillet et al., 2002; Ali et al., 2012), and RDA analysis has revealed a positive relationship between $Char_{accum}$ and Poaceae and a negative relationship between $Char_{accum}$ and Chenopodiaceae (Fig. 4, Supplement Table 1). Following grassland records, however, total charcoal at Shenkani, should represent fires <5 km from the core area and local area burnt (Aleman et al., 2013; Leys et al., 2015). This suggests that Poaceae was the primary fuel driving these local fires and that decreases in Poaceae and increases in Chenopodiaceae resulted in the reduction of fire episodes and are reflective of local steppe change.

5.2. Human activities

Pollen and non-pollen palynomorphs suggest limited evidence of human impact on our record. At Shenkani, *Cerealia*-type pollen is found throughout and is likely related to wild species in the early Holocene. Linking this pollen-type with agriculture in southwest

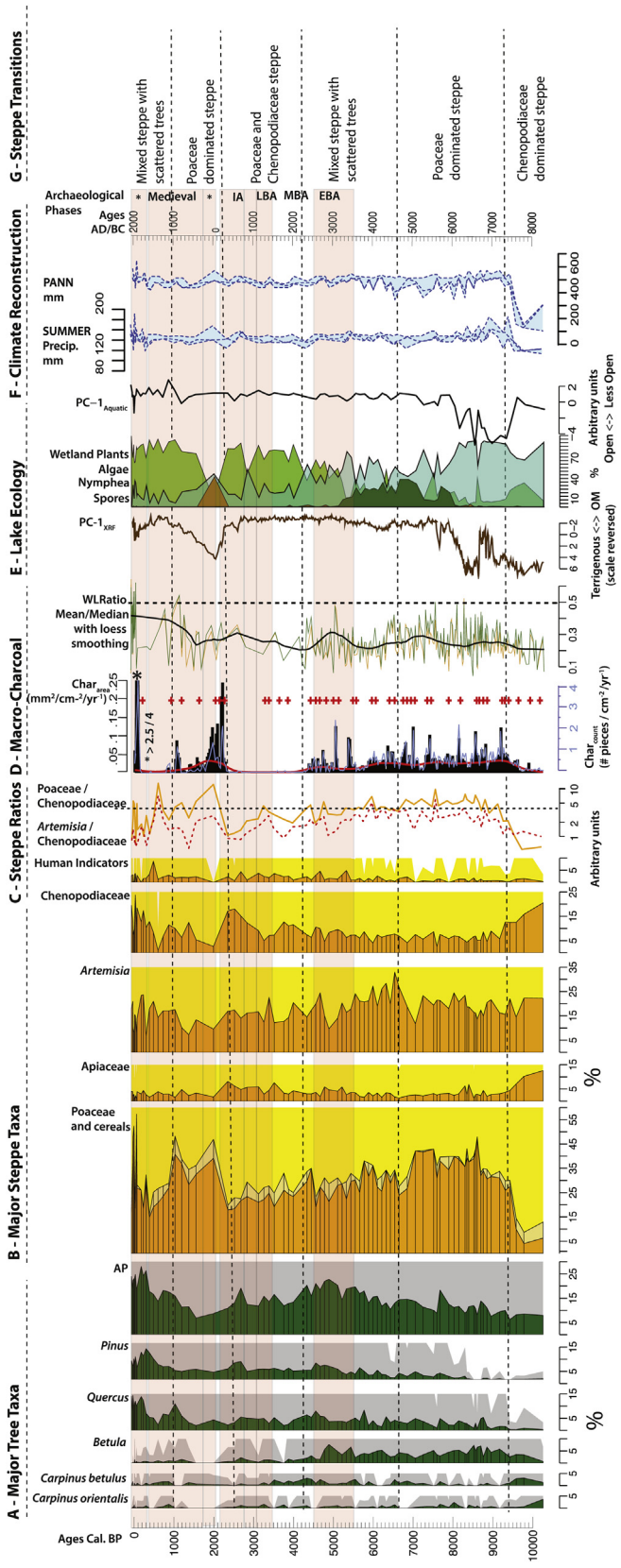

Fig. 5. Select proxies arranged by age A.) Major arboreal pollen B.) Major herb taxa and human indicator pollen (human indicators include *Plantago*, *Rumex*, *Sanguisorba, and Cichorioideae*) C.) Ratios of Poaceae/Chenopodiaceae (P/C) and *Artemisia*/Chenopodiaceae (*A*/C) from percentage data plotted with a logarithmic scale. Mean value of P/C represented by the line. D.) Macro-charcoal results displayed in charcoal accumulation ($Char_{accum}$) rates by area (black) and count (blue). Peak values are red crosses from CharAnalysis. The red line separates background and noise to calculate peaks. W/L ratio plot of the mean (green) and median (brown) for charcoal particles for a sample. The black line is loess smoothing of charcoal particles WL measurments displayed for clarity (span = .12, delta = 0.95). E.) XRF plot of PC-1 from PCA_{xrf} analysis. Plot of aquatic taxa and spores. Spores (brown), *Nymphea* (dark green), algae (blue-green), macrophytes (green). Plot of aquatic pollen and algae from PC-$1_{aquatic}$. F.) Climate reconstruction P_{summer}, P_{ANN} G.) Revised chronology of archaeological settlement periods on the Tsaghkahovit plain (Manning et al., 2018; Franklin, 2014a). * Denotes Antiquity and Modern period. Lastly, major steppe transitions. (For interpretation of the references to colour in this figure legend, the reader is referred to the Web version of this article.)

Asia and the Caucasus is complicated by the presence of wild grass species, related to modern cereals, which produce *Cerealia*-type pollen (Bottema and Woldring, 1990). This is the same for other steppe taxa, such as *Rumex*, Caryophyllaceae, and Chenopodiaceae, which are often utilized as anthropogenic indicators (Behre, 1981). At Shenkani, these pollen types are found in records prior to known regional agriculture (see Hovsepyan and Willcox, 2008 for early agriculture examples). However, results from RDA (Fig. 4) suggest that cereals have a moderate correlation with periods of human occupation. Although dung-inhabiting fungal spores, such as *Sporormiella*, do indicate the presence of large herbivores (Van Geel, 2002), at Shenkani they are primarily found during periods of low Cyperaceae and open water. This suggests that during periods when tussocks covered the wetland, Cyperaceae might have blocked *Sporormiella*'s deposition. This is because spores are usually deposited near the site of sporulation (Van Geel, 2002).

5.3. Holocene record of steppe and treeline transitions

5.3.1. Early holocene steppe transition

The early Holocene record at Shenkani begins with an open arid landscape characterized by Chenopodiaceae-*Artemisia* steppes (Fig. 5). This vegetation is distinctive of the Younger Dryas (12.9–11.7 ka) in the Eastern Mediterranean (Rossignol-Strick, 1995) and today is found in semi-desert areas located at lower altitudes (480–1200 m a.s.l) (Fig. 1c; Vegetation zones N7; O8 in Bohn et al., 2000) where precipitation is 200–400 mm annually (Fig. 1c; Volodicheva, 2002). These similarities in vegetation suggest the early Holocene landscape was more arid than today. Although the beginning of the record is primarily dominated by xeric steppe vegetation, stands of *Carpinus betulus* and *Carpinus orientalis* were also present. According to Connor and Kvavadze (2008), a similar composition of semi-desert steppes (*Carpinus*, *Ostrya*-type, Chenopodiaceae, *Artemisia*, *Ephedra*) occurred during the early Holocene between 1500 and 1900 m a.s.l in Georgia. This composition may resemble today's mixed open woodlands and herbaceous areas of southern Georgia, characteristic of a dry and cold climate (Nakhutsrishvili, 2013).

Around 9500 cal. BP, a shift in steppe vegetation occurred, as the sudden spread of Poaceae replaced Chenopodiaceae and *Artemisia* as the dominant steppe taxon (although *Artemisia* remained stable) establishing a grassland landscape. This expansion appears to have been part of a pioneering phase recorded at different times in pollen records across the Caucasus and southwest Asia (see Messager et al., 2017 for discussion) and points to increased moisture availability. Today, Poaceae dominates true and herb-grass steppes areas in Armenia that are associated with annual precipitation between 400 and 600 mm annually (Fig. 1).

This transition from Chenopodiaceae to Poaceae is marked by two erosional phases, with increased terrigenous endmembers into the catchment between 10240 - 8870 and 8550–8000 cal. BP (Fig. 6). Manganese (Mn), which is an indicator of redox conditions and bottom-water oxygenation (Calvert and Pedersen, 1993),

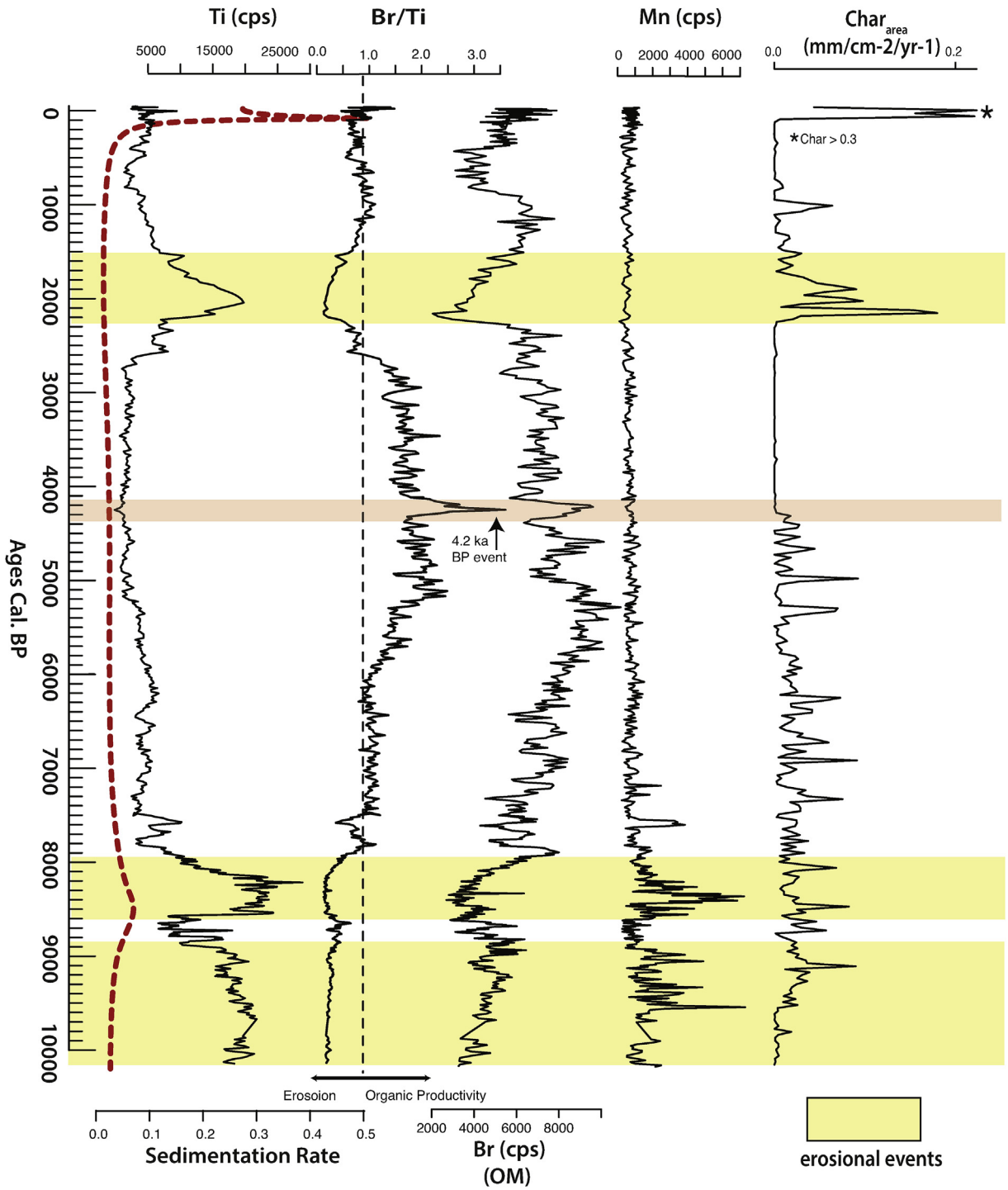

Fig. 6. Select XRF data graphed by age. Shenkani's sedimentation rates ($cm.yr^{-1}$) along with an XRF ratio of (Br/Ti) with the mean indicated with a dotted black line. XRF counts per a second (CPS) for Ti, Br, Mn graphed alongside $Char_{accum}$ rates for $Char_{area}$. Periods of increased erosion are highlighted.

increases during both erosional events. This change in redox conditions may be linked with increased precipitation that facilitated erosion into the catchment, leading to re-oxygenation of bottom waters associated with terrigenous deposits (Sabatier et al., 2017). Unstable precipitation, which is recorded in the pollen climate reconstructions from Zarishat, Armenia (Joannin et al., 2014) during this time, may have contributed to redox conditions. The spread of Poaceae appears to stabilize the surrounding and catchment during this first erosional event (Fig. 5) as shown in decreased erosion in MS (Fig. 3). This second erosion event is not marked by a vegetation change and does not have a clear cause. Similar periods of erosion are recorded regionally at Zarishat, Armenia (Joannin et al., 2014), and Lake Paravani, Georgia, which Messager et al. (2013) posit might be linked to active local glaciers. The regionality of this event suggests a possible linkage with the 8.2 ka event. These events begin to subside with the spread of aquatic and semi-aquatic taxa in the watershed at 8200 cal. BP.

The expansion of Poaceae is also accompanied by increased

charcoal accumulation. Although fires were present prior to 9500 cal. BP, the increase in biomass created by the spread of Poaceae as well as an increase in precipitation may have enabled a greater fuel source. In the North American prairies (Leys et al., 2017) and the savannas of the Afrotropics (Aleman et al., 2013), modern studies investigating the relationship between sedimentary charcoal and landcover have found linkages between precipitation, increased tall-grass biomass, and fire frequency. RDA analysis (Fig. 4) suggests a cyclical relationship between local fires and Poaceae, where Poaceae biomass increases drove fuel, and fires, in turn, maintained the grassland. Periods of alternating moisture (to increase fine fuel biomass) and aridity (to dry vegetation for ignition) are also necessary for sustained fire activity (McPherson, 1995) and must have occurred throughout the Holocene. These periods of alternating precipitation and aridity occur around Shenkani today, with high spring precipitation that transitions into dry late summers (Fig. 1b), although most fires today are the result of human ignition (Zibtsev et al., 2013).

In the Caucasus, select Poaceae species can grow on the wetland itself, increasing Poaceae's signal. This was discussed in relation to sequences from Vanevan, Armenia (Leroyer et al., 2016), and in Georgia (Connor, 2011). The transition from Chenopodiaceae to Poaceae occurs at different timings than wetland transitions, with the spread of Poaceae occurring at 9500 cal. BP. Changes in wetland OM lag behind this and are established at 8200 cal. BP. The spread of Cyperaceae tussocks marks the transition to a full wetland with aquatic plants at 5500 cal. BP (Fig. 3). This, along with the regional scale of Poaceae expansion during the early Holocene (Messager et al., 2017), suggests that Poaceae is established on the surrounding landscape rather than in the wetland during this time.

5.3.2. Mid-holocene tree encroachment and Betula's decline

In the mid-Holocene trees begin to encroach onto the steppe landscape. During this period, AP increased, reaching its maximum for the early and mid-Holocene, both in terms of percentage (<23%) and composition between 6000 and 4700 cal. BP. At this time, both mesophilic taxa (*Quercus, Fagus, Fraxinus, Carpinus, Tilia,* and *Ulmus*), and boreal species (*Pinus* and *Betula*), were represented. The similar arboreal percentage (24%) to the sediment at the top of the core suggests a patchy mosaic of trees growing on the landscape similar to today's configuration. As trees encroached, increases in Chenopodiaceae and various herbs (Scrophulariaceae, *Rumex*, Fabaceae) also points to a more mixed steppe landscape. A slight increase in the W/L ratio (Fig. 5d) at 5000 cal. BP suggests that woody biomass fuel may have made a small contribution to fires during this time. However, a mean W/L ratio <0.5, low AP percentages, and relationship between $Char_{accum}$ and Poaceae in RDA (Fig. 4), suggests that Poaceae and herbs constituted biomass fuel (See Aleman et al., 2013; Leys et al., 2017). Trees were also not located around the basin and fires may have inhibited their establishment. This is because, certain fire cycles can kill surface seeds or prevent young trees from reaching resprouting age (McPherson, 1995; Merola-Zwartjes, 2004). In addition, a similar mosaic of trees found today in the Kasakh valley suggests a slow recolonization process. This spread of trees is indicative of increased temperature and precipitation amendable to tree growth, during a period that others have suggested as a climate optimum (Wick et al., 2003; Connor and Kvavadze, 2008; Messager et al., 2013). In the wetland, decreases in terrigenous endmembers at 7700 cal. BP, with additional decreases at 6000 cal. BP and increases in OM at 7900 cal. BP followed by increases in the Br/Ti ratio at 6000 cal. BP (Fig. 6), suggests the onset of climatic stability amendable to mire productivity and tree growth. This corresponds to the mid-Holocene arboreal pollen maximum.

At Shenkani, a drop in *Betula* at 4700 cal. BP marks an early transition from the mid- to the late Holocene, followed by declines in *Quercus* and *Pinus,* and fire intensities after 4200 cal. BP. The positioning of *Betula* and Poaceae at opposite poles of other tree taxa (*Quercus*, *Pinus*, etc) across PC-1 (Fig. 4) suggests possible vegetation dynamics related to multiple factors, including human activity, vegetation competition, and climate. Although the timing varies, the rise of *Betula* and subsequent decline is prevalent in regional records (Iran, Lake Urmia: Bottema, 1986; Turkey, Lake Van: Wick et al., 2003; Litt et al., 2009; Armenia, Vanevan peat: Leroyer et al., 2016; Georgia, Lake Aligol: Connor, 2011). Since it is a light-demanding species (Connor, 2011), vegetation competition amongst arboreal species has been implicated in its disappearance in Turkey (Bottema and Woldring, 1984). At Shenkani, however, the low amounts of arboreal pollen, in conjunction with *Betula* reaching its maximum at the height of the mid-Holocene tree expansion, suggest that vegetation competition played a limited role.

Instead, a likely combination of climate and human activities most likely drove its disappearance. Human activities, including wood acquisition and pastoralism, have been extensively recorded at the EBA settlements on the Tsaghkahovit plain and in the Kasakh valley, attesting to a thriving mixed agro-pastoral economy (Hovsepyan, 2008; Monahan, 2008). At the archaeological site of Gegharot, approximately 10 km north of Shenkani, excavated charcoal remains have revealed the acquisition of *Betula* by EBA communities (Jude et al., 2016).

Although humans likely contributed to *Betula's* decline, increasing aridity may have prohibited its regrowth. According to Варданян and Мхитарян (2018), several species of *Betula* (*B. litwinowii, B. pendula*) grow today in Armenia's sub-alpine zones (1400–2700 m a.s.l) as crooked forests. According to them, forest expansions in these areas are limited by multiple factors, including short cold summer growing seasons, cold winters, and limited precipitation. Increasing aridity is attested too in the isotope record from Lake Van during this period (Wick et al., 2003). This suggests that before 4700 cal. BP, climate conditions may have fostered *Betula's* growth, but after that time, anthropogenic activities and aridity led to its decline.

5.3.3. The 4.2 ka BP event

The 4.2 ka BP event is regularly discussed in the paleoclimate and archaeological literature across the Mediterranean Basin and beyond (Cullen et al., 2000; Staubwasser and Weiss, 2006; Kaniewski et al., 2018; Bini et al., 2019) and has been used to delineate the transition from the mid- to late Holocene. Walker et al. (2012), bases this division on isotope records from Mawmluh Cave KM-A, India, linked with a two-phased (with shifts at 4.3, 4.1, and a mid-point between the two events at 4.2 ka) mid- to low-latitude aridity event lasting for ~375 modeled years. To date, this event has not been recorded in the Southern Caucasus pollen records. However, periods of increased aridity are recorded from dust influxes at Lake Neor in northwestern Iran around 4200 cal. BP (Sharifi et al., 2015) and in pollen and isotope records from Lake Van (Wick et al., 2003). Although there is no clear indication of this event in Shenkani's pollen record, an increase in the Br/Ti ratio (Fig. 6) shows a decrease in terrigenous inputs and an increase in organic productivity between 4300 and 4100 cal. BP, which might be related. Additional high-resolution records across the Caucasus will hopefully elucidate this further.

5.3.4. Late holocene steppe transitions

At Shenkani, the late Holocene onset is marked by an arboreal decline (~4200 cal. BP), but steppe transitions are less pronounced. To understand these changes, we split the late Holocene into 3 steppe transitions: i.) herbaceous Chenopodiaceae steppe (4200–2500 cal. BP) ii.) Poaceae/*Artemisia* steppe (2500–1000 cal.

BP) iii.) mixed steppe with arboreal and anthropogenic elements (1000 cal. BP – present). Steppe transition i.) begins in the mid-Holocene but, declines in arboreal pollen after 4200 cal. BP accelerate this change. Here, increases in pollen are primarily associated with Chenopodiaceae, and other herbaceous steppe taxa (Lamiaceae, Caryophyllaceae, *Thalictrum*), while decreasing values are associated with Poaceae, *Artemisia,* and arboreal taxa (*Quercus*, *Pinus*). Aridity has been recorded in Central Asia beginning at 6000 cal. BP (Chen et al., 2008), in the stacked isotope records from southwest Asia from 3000 cal. BP (Roberts et al., 2011), and at Zarishat, Armenia from 3000 cal. BP (Joannin et al., 2014). Both steppe ratios (Fig. 5, P/C, and *A*/C) follow similar decreasing trends, suggesting local aridity (El-Moslimany, 1990).

This change appears to have fostered the spread of Chenopodiaceae, and led to declines in Poaceae, reducing local fire activity at 4200 cal. BP. Although fires will initially eliminate grasses in the short-term, in the long term these same fires promote grassland rejuvenation and prevent the encroachment of trees and shrubs (McPherson, 1995; Merola-Zwartjes, 2004). Grassland fires, however, are dependent on biomass, and precipitation change (McPherson, 1995), and grazing can reduce fuel load and fire frequencies (Archer, 1989; Merola-Zwartjes, 2004). The negative correlation with Chenopodiaceae and $Char_{accum}$ (Fig. 4) suggests that this reduction in fine fuel biomass and an increase in aridity drove these declines. Grazing has also been implicated in the conversion of grasslands to shrublands (Archer, 1989; Merola-Zwartjes, 2004), and can lead to the spread of Chenopodiaceae due to its low forage value and toxicity (Wesche and Treiber, 2012). The role of humans remains elusive during this period due both to the paucity of recorded Middle Bronze Age archaeological sites (Smith et al., 2009; Sagona, 2017) and the overall low concentration of *Sporormiella* in our record, future archaeological investigations will no doubt elucidate this connection further.

Transition ii.) occurred after a short rebound of arboreal taxa at 2800 cal. BP, followed by its subsequent decline and an increase in Poaceae and fire. Here, Poaceae increases in our pollen diagram, while arboreal pollen (*Quercus*, *Pinus*, *Betula*) and xeric taxa (Chenopodiaceae, Caryophyllaceae) decrease. At 2600 cal. BP, a series of events denotes a drying event. First, this presents itself as a small erosion event (increases in Ti, Al, etc), followed by an increase in charcoal accumulations. Then, there is a decrease in OM (LOI), an increase in terrigenous inputs (Ti, Al, etc), indicating a sizable erosion event, and the spread of Poaceae. These episodes point to the initial drying of the wetland, followed by the invasion of fire. In this instance, fire predates the return of Poaceae and corresponds to a decrease in aquatic taxa percentages which are then replaced by spores (Fig. 5). This suggests a fire perturbation of the wetland system and a local expansion of Poaceae. Multiple sources have also noted that fire events linked with erosion indicate catchment fires (Whitlock and Larsen, 2002; Leys et al., 2016).

Although the timing varies, the opening of the landscape and increased fire activity are not localized to Shenkani (Fig. 7), and have been recorded at Zarishat, Armenia (Joannin et al., 2014), and Lake Imera, Georgia (Connor, 2011). At Zarishat, fires invaded the lakebed and resulted in the decline of Cyperaceae at 2200-1500 cal. BP (Joannin et al., 2014). At Imera, Connor (2011) suggests that fires between 2400 and 1700 cal. BP significantly modified the arboreal landscape. At Lake Van, Turkey, oxygen isotopes continue to record increasing aridity, a trend starting at the beginning of the late Holocene, which reverses around 2000 cal. BP (Fig. 7) (Wick et al., 2003). This reversal also occurs at Shenkani at this time, attested to by the decreases in terrigenous endmember inputs (XRF, MS), increases in organic matter, and a slight rise in sedimentation (Fig. 6). This suggests a gradual transition back to a wetland. Trees return to the Kasakh valley at 1400 cal. BP, dominated by *Quercus*.

The last steppe transition iii.) occurred from 1000 cal. BP – to the present and is characterized by increased arboreal pollen and a mixed steppe landscape. Although anthropogenic pollen indicators can be ambiguous in steppe landscapes (see section 5.2), there is a jump in this pollen type at 600 cal. BP. Before this, a decline of *Quercus* between 1000 and 600 cal. BP is coupled with a decrease in Poaceae grasslands and the spread of *Artemisia,* suggesting these events might be linked. Human activity is well documented in both archaeological and epigraphic sources in the Kasakh valley. Especially during the late medieval period (12th – 15th c. AD/900–500 cal. BP) (Smith et al., 2009; Franklin, 2014b). These connections suggest that humans most likely contributed to changes in both arboreal and steppe taxa over the past 1000+ years, co-creating this mixed steppe landscape. A higher resolution pollen sediment core currently undergoing analysis taken from a wetland (2058 m a.s.l) adjacent to a multi-period archaeological site will hopefully further elucidate the nuances between these relationships further.

5.4. Steppe maintenance and afforestation

Holocene steppe changes at Shenkani both correspond and diverge from traditional climatic transitions across the South Caucasus and southwest Asia (Fig. 7). The vegetation at the onset of the early Holocene at Shenkani is primarily xeric (Chenopodiaceae, *Artemisia*), mirroring regional records from Turkey (Van Zeist et al., 1975; Wick et al., 2003; Litt et al., 2009), Iran (Bottema, 1986; Djamali et al., 2008), the South Caucasus (Messager et al., 2013, 2017; Montoya et al., 2013; Joannin et al., 2014), Black Sea (Shumilovskikh et al., 2012), and into Central Asia (Wright et al., 2003). As discussed in Messager et al. (2017), the expansion of a pioneering phase of Poaceae is followed by afforestation in many of these records (Lake Van, Turkey, Wick et al., 2003; Lake Nariani, Georgia, Messager et al., 2017; Lake Mirabad & Lake Zeribar, western Iran Van Zeist and Bottema, 1977). Unlike the above, however, sequences from Armenia including Shenkani, Zarishat (Joannin et al., 2014), Vanevan Peat (Leroyer et al., 2016), and from Lake Urmia, Iran (Bottema, 1986) remain primarily steppe. But what were the forces that contributed to this persistent Holocene steppe?

Overall, the early Holocene steppe transformations at Shenkani at 9500 cal. BP is roughly synchronous with treeline expansions recorded in Georgia (Messager et al., 2013, 2017), but lag behind the Poaceae expansions, suggesting that similar climate mechanisms that prompted the establishment of trees also led to shifts to grasslands. These mechanisms include shifts in seasonal precipitation, which are clearly stated in the reconstruction from Zarishat, Armenia (+91 mm in spring precipitation at the early-mid Holocene transition; Joannin et al., 2014), and increases in moisture, recorded in Lake Van's isotope record (Wick et al., 2003). Shenkani's reconstruction also records an increase in precipitation at this time (Fig. 5). At Shenkani, climate, specifically precipitation, appears to be the primary factor limiting the spread of trees and driving shifts in vegetation throughout the Holocene. Today, steppe areas in Eurasia are found between humid boreal forest and arid deserts (Chibilyov, 2002). Shifts in precipitation, therefore, can dictate the number of trees and vegetation type on these steppe landscapes. At Shenkani, precipitation was the primary factor limiting afforestation while also prompting shifts between Poaceae and Chenopodiaceae dominated steppes.

This, however, is not the only mechanism controlling the steppe landscape. Fires also play an important role in limiting trees in these transitional environments by destroying tree seeds and seedlings (McPherson, 1995; Merola-Zwartjes, 2004) prior to their establishment or migration. Tall grasses can also block woodland

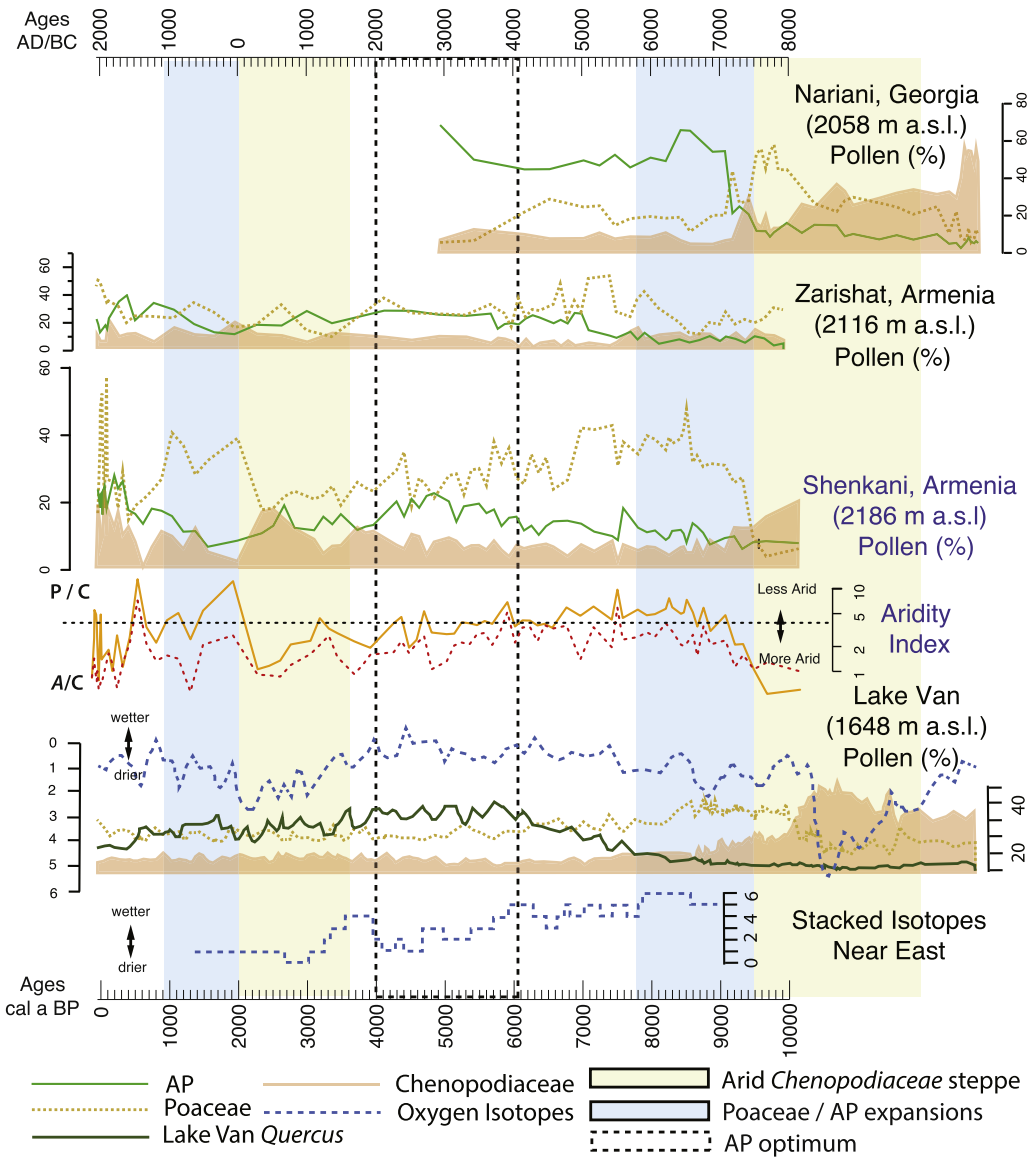

Fig. 7. Regional records in Armenia, Georgia, and Turkey. Select pollen diagrams of Poaceae, Chenopodiaceae, and AP from Lake Nariani (Messager et al., 2017), Zarishat (Joannin et al., 2014), Shenkani (this study), and Lake Van (AP line for Lake Van represents only *Quercus*) (Wick et al., 2003). The steppe/aridity index is from this study and represents a Poaceae/Chenopodiaceae (P/C) and *Artemisia*/Chenopodiaceae (A/C) ratio plotted on a logarithmic scale (methods, 3.3). Oxygen isotopes are included in Lake Van diagram (Wick et al., 2003) and stacked isotope records from southwest Asia are illustrated below (Roberts et al., 2011).

seedlings through both above and below ground competition (Volodicheva, 2002). At Shenkani, while increases in precipitation during the mid-Holocene might have been able to foster tree expansion, locally, these fires and tall grasses prevented tree establishment and migration. Fires fueled by both climate and aided by human ignition have also been implicated as a possible explanation for the delays in oak expansion in southwest Asia (Roberts, 2002; Turner et al., 2008, 2010). At the end of the mid-Holocene, however, fires were no longer the primary mechanism for maintaining this steppe. Instead, aridity drove Poaceae biomass down, leading to declines in fires, and also declines in trees.

Humans have also contributed to the disappearance of the limited trees on the landscape particularly during the mid-Holocene by Early Bronze Age communities and in the Late Medieval period. Grazing most likely also influenced the spread of Chenopodiaceae and the decline of grasses during the Middle and Late Bronze Age, but more research is needed to understand the extent. At Shenkani, however, there is limited evidence that human communities were responsible for extensive deforestation and conversion of this landscape to an open steppe as has been historically proposed for some areas of the Caucasus (Volodicheva, 2002; Nakhutsrishvili, 2013). Instead, climate, specifically precipitation, is the primary mechanism maintaining this Holocene steppe landscape with fires and humans contributing to its maintenance.

6. Conclusion

This paper has challenged regional narratives that human activities drove deforestation and steppe conversion in the Holocene. Instead, evidence from the Shenkani wetland indicates that this area has remained a steppe with small stands of trees throughout the available record. Climate appears to have been the primary driver of change, although fire, fueled by Poaceae biomass, has been important in maintaining this landscape, especially during early

and mid-Holocene grassland expansions. More research is needed to fully understand how human activities contributed to change; however, changes during the Early Bronze Age and Late Medieval period appear to be at least partially driven by humans. Changes in arboreal pollen also signal climatic changes primarily during the mid- to late Holocene transition. This record from Shenkani augments our knowledge of the South Caucasus region and improves our understanding of the mechanisms of steppe transformation and maintenance over time.

Funding

Financial support for this study was provided by two French-Armenian International Associated Laboratories: HEMHA (Humans and environments in mountainous habitats, the case of Armenia; supervised by C. Chataigner and P. Avetisyan) and LIA NHASA (Natural Hazards and Adaptation Strategies in Armenia, from 10,000 BC onwards; supervised by B. Perello and A. Karakhanyan). These programs between Armenia and France are funded by the French National Centre for Scientific Research (CNRS, France). Additional financial support was provided by two National Science Foundation (USA) grants for Project ArAGATS (BCS-1561237 PIs: Ian Lindsay, Alan Greene, Maureen Marshall and BCS-1561240 PIs: Lori Khatchadourian and Adam T, Smith) and through a National Science Foundation Graduate Research Fellowship (DGE-1650441) for A. Cromartie. Research and writing of this manuscript occurred at the Institut des Sciences de l'Evolution de Montpellier at the University of Montpellier on a Chateaubriand, Make our Planet Great Again fellowship for the humanities and social sciences from the Embassy of France in the United States and a MUSE explore grant from I-site MUSE (France), University of Montpellier for A. Cromartie.

Author contribution

Amy Cromartie: Conceptualization, Methodology, Investigation, Formal analysis, Writing - original draft, Writing - review & editing, Funding acquisition. Claire Blanchet: Investigation, Formal analysis, Writing & Review. Chéïma Barhoumi: Investigation, Formal analysis, Writing & Review. Erwan Messager: Conceptualization, Formal analysis, Supervision; Validation. Writing - review & editing. Odile Peyron: Conceptualization, Formal analysis, Supervision; Validation. Writing - review & editing. Vincent Ollivier: Resources, Writing - review & editing. Pierre Sabatier: Conceptualization, Formal analysis, Supervision; Validation. Writing - review & editing. David Etienne: Resources, Writing - review & editing. Arkady Karakhanyan: Resources, Review, Funding acquisition. Lori Khatchadourian: Supervision, Resources, Writing - review & editing, Funding acquisition, Adam T. Smith: Supervision, Resources, Writing - review & editing, Funding acquisition, Ruben Badalyan: Resources, Review, Funding acquisition. Bérengère Perello: Resources, Review, Funding acquisition. Ian Lindsay: Resources, Review, Funding acquisition. Sebastien Joannin: Project administration, Conceptualization, Methodology, Supervision, Formal analysis, Investigation, Validation, Writing - review & editing, Funding acquisition.

Declaration of competing interest

The authors declare that they have no known competing financial interests or personal relationships that could have appeared to influence the work reported in this paper.

Acknowledgements

The authors would like to express their appreciation for help with the sediment and geochemical analysis by Adrien Jacquier and for pollen sample preparation by Sandrine Canal. We would also like to thank Samuel Nahapetyan for his assistance with fieldwork and Lucas Dugerdil and Mary Robles for contributing pollen surface samples linked to our climate reconstruction. We would like to thank Gabrielle Borenstein for comments on an earlier draft of this manuscript and to Simon Connor for his constructive comments which greatly improved this manuscript. We also want to thank Alan Greene, Maureen Marshall, Christine Chataigner, and Pavel Avetisyan for helping to fund this research. This is ISEM publication n°: ISEM 2020-174.

Appendix A. Supplementary data

Supplementary data to this article can be found online at https://doi.org/10.1016/j.quascirev.2020.106485.

References

Akhani, H., Djamali, M., Ghorbanalizadeh, A., Ramezani, E., 2010. Plant biodiversity of Hyrcanian relict forests, N Iran: an overview of the flora, vegetation, palaeoecology and conservation. Pakistan J. Bot 42, 231–258.

Aleman, J.C., Blarquez, O., Bentaleb, I., Bonté, P., Brossier, B., Carcaillet, C., Gond, V., Gourlet-Fleury, S., Kpolita, A., Lefèvre, I., Oslisly, R., Power, M.J., Yongo, O., Bremond, L., Favier, C., 2013. Tracking land-cover changes with sedimentary charcoal in the Afrotropics. The Holocene 23, 1853–1862. https://doi.org/10.1177/0959683613508159.

Ali, A.A., Blarquez, O., Girardin, M.P., Hély, C., Tinquaut, F., El Guellab, A., Valsecchi, V., Terrier, A., Bremond, L., Genries, A., Gauthier, S., Bergeron, Y., 2012. Control of the multimillennial wildfire size in boreal North America by spring climatic conditions. Proc. Natl. Acad. Sci. Unit. States Am. 109, 20966–20970. https://doi.org/10.1073/pnas.1203467109.

Archer, S., 1989. Have southern Texas savannas been converted to woodlands in recent history? Am. Nat. 134, 545–561.

Arimura, M., Gasparyan, B., Chataigner, C., 2012. Prehistoric sites in Northwest Armenia: Kmlo-2 and Tsaghkahovit. In: Matthews, R.J., Curtis, J. (Eds.), Proceedings of the 7th International Congress of the Archaeology of the Ancient Near East. Volume 3: Fieldwork and Recent Research – Posters. Harrasowitz, Wiesbaden, pp. 135–150.

Arnaud, F., Révillon, S., Debret, M., Revel, M., Chapron, E., Jacob, J., Giguet-Covex, C., Poulenard, J., Magny, M., 2012. Lake Bourget regional erosion patterns reconstruction reveals Holocene NW European Alps soil evolution and paleohydrology. Quat. Sci. Rev. 51, 81–92. https://doi.org/10.1016/j.quascirev.2012.07.025.

Atalay, I., Efe, R., 2010. Structural and distributional evaluation of forest ecosystems in Turkey. J. Environ. Biol. 31, 61–70.

Badalyan, R.S., Avetisyan, P., 2007. Bronze Age and Early Iron Age archaeological sites in Armenia. I. Mt Aragats and its surrounding region, BAR International Series 1697. In: Archaeopress, Oxford.

Badalyan, R., Smith, A.T., Lindsay, I., Khatchadourian, L., Avetisyan, P., 2008. Village, fortress, and town in Bronze and Iron Age Southern Caucasia: a preliminary report on the 2003–2006 investigations of Project ArAGATS on the Tsaghkahovit plain, Republic of Armenia. Archaol Mitteilungen aus Iran und Turan 40, 45–105.

Badalyan, R., Smith, A.T., Lindsay, I., Harutyunyan, A., Greene, A., Marshall, M.E., Monahan, B., Hovsepyan, R., 2014. A preliminary report on the 2008, 2010, and 2011 investigations of Project ArAGATS on the Tsaghkahovit plain, Republic of Armenia. Archaol. Mitteilungen aus Iran und Turan 46, 149–222.

Bajard, M., Sabatier, P., David, F., Develle, A.-L., Reyss, J.-L., Fanget, B., Malet, E., Arnaud, D., Augustin, L., Crouzet, C., Poulenard, J., Arnaud, F., 2016. Erosion record in Lake La Thuile sediments (Prealps, France): evidence of montane landscape dynamics throughout the Holocene. The Holocene 26, 350–364. https://doi.org/10.1177/0959683615609750.

Behre, K.E., 1981. The interpretation of anthropogenic indicators in pollen diagrams. Pollen Spores 23, 225–245.

Beug, H.-J., 2004. Leitfaden der Pollenbestimmung für Mitteleuropa und angrenzende Gebeite. Pfeil, München.

Bini, M., Zanchetta, G., Perşoiu, A., Cartier, R., Català, A., Cacho, I., Dean, J.R., Di Rita, F., Drysdale, R.N., Finnè, M., Isola, I., Jalali, B., Lirer, F., Magri, D., Masi, A., Marks, L., Mercuri, A.M., Peyron, O., Sadori, L., Sicre, M.-A., Welc, F., Zielhofer, C., Brisset, E., 2019. The 4.2 ka BP Event in the Mediterranean region: an overview. Clim. Past 15, 555–577. https://doi.org/10.5194/cp-15-555-2019.

Blaauw, M., 2010. Methods and code for "classical" age-modelling of radiocarbon sequences. Quat. Geochronol. 5, 512–518. https://doi.org/10.1016/j.quageo.2010.01.002.

Blanchet, C., 2017. Reconstitution paléoenvironnementale et paléoclimatique à partir de l'étude conjointe des pollens et des palynomorphes non-polliniques (NPP) de la zone humide de Shenkani en Arménie. Thesis Masters. Université de Montpellier.
Bohn, U., Gollub, G., Hettwer, C., 2000. Karte der natürlichen Vegetation Europas. Bundesamt für Naturschutz, Bonn.
Bottema, S., 1986. A late quaternary pollen diagram from Lake Urmia (northwestern Iran). Rev. Palaeobot. Palynol. 47, 241–261.
Bottema, S., Woldring, H., 1984. Late Quaternary vegetation and climate of southwestern Turkey. Part II. Palaeohistoria 26, 123–149.
Bottema, S., Woldring, H., 1990. Anthropogenic indicators in the pollen record of the Eastern Mediterranean. In: Bottema, S., Entjes-Nieborg, G., Van Zeist, W. (Eds.), Man's Role in the Shaping of the Eastern Mediterranean Landscape. A.A. Balkema, Rotterdam, pp. 231–264.
Варданян, Ж.А., Мхитарян, А.К., 2018. Древесные растения и дендроценозы субальпийской зоны Северо-восточной Армении. Biological J. Armen. Биологический Журнал Армении. Հայաստանի կենսաբանական հանդես 70, 45–51.
Calvert, S.E., Pedersen, T.F., 1993. Geochemistry of Recent oxic and anoxic marine sediments: implications for the geological record. Mar. Geol. 113, 67–88. https://doi.org/10.1016/0025-3227(93)90150-T.
Carcaillet, C., Almquist, H., Asnong, H., Bradshaw, R.H.W., Carrión, J.S., Gaillard, M.-J., Gajewski, K., Haas, J.N., Haberle, S.G., Hadorn, P., Müller, S.D., Richard, P.J.H., Richoz, I., Rösch, M., Sánchez Goñi, M.F., von Stedingk, H., Stevenson, A.C., Talon, B., Tardy, C., Tinner, W., Tryterud, E., Wick, L., Willis, K.J., 2002. Holocene biomass burning and global dynamics of the carbon cycle. Chemosphere 49, 845–863.
Chataigner, C., Badalyan, R., Arimura, M., 2014. The Neolithic of the Caucasus. In: Oxford Handbooks Online. Oxford University Press, doi:10.1093/oxfordhb/9780199935413.013.13.
Chen, F., Yu, Z., Yang, M., Ito, E., Wang, S., Madsen, D.B., Huang, X., Zhao, Y., Sato, T., Birks, H.J.B., Boomer, I., Chen, J., An, C., Wünnemann, B., 2008. Holocene moisture evolution in arid central Asia and its out-of-phase relationship with Asian monsoon history. Quat. Sci. Rev. 27, 351–364. https://doi.org/10.1016/j.quascirev.2007.10.017.
Chernyshev, I., Lebedev, V., Arakelyants, M., Jrbashyan, R., Gukasyan, Y., 2002. Quaternary geochronology of the Aragats volcanic center, Armenia: evidence from K-ar dating. Dokl. Earth Sci. 384, 393–398.
Chibilyov, A., 2002. 11 steppe and forest-steppe. In: Shahgedanova, M. (Ed.), The Physical Geography of Northern Eurasia. Oxford University Press, Oxford, pp. 248–266.
Colombaroli, D., Tinner, W., Van Leeuwen, J., Noti, R., Vescovi, E., Vannière, B., Magny, M., Schmidt, R., Bugmann, H., 2009. Response of broadleaved evergreen Mediterranean forest vegetation to fire disturbance during the Holocene: insights from the peri-Adriatic region. J. Biogeogr. 36, 314–326.
Connor, S.E., 2011. A promethean legacy: late quaternary vegetation history of southern Georgia, the Caucasus. Peeters, Leuven.
Connor, S.E., Kvavadze, E.V., 2008. Modelling late Quaternary changes in plant distribution, vegetation and climate using pollen data from Georgia. Caucasus. J. Biogeogr 36, 529–545.
Croudace, I.W., Rothwell, R.G., 2015. Micro-XRF Studies of Sediment Cores: Applications of a Non-destructive Tool for the Environmental Sciences. Springer, Dordrecht.
Cullen, H.M., deMenocal, P.B., Hemming, S., Hemming, G., Brown, F.H., Guilderson, T., Sirocko, F., 2000. Climate change and the collapse of the Akkadian empire: evidence from the deep sea. Geology 28, 379–382. https://doi.org/10.1130/0091-7613(2000)28<379:CCATCO>2.0.CO;2.
Davoyan, M.O., 1971. Area of modern glaciation on Mt. Aragats and the diminution of firn basins. Int. Geol. Rev. 13, 530–533. https://doi.org/10.1080/00206817109475464.
Djamali, M., de Beaulieu, J.-L., Shah-hosseini, M., Andrieu-Ponel, V., Ponel, P., Amini, A., Akhani, H., Leroy, S.A.G., Stevens, L., Lahijani, H., Brewer, S., 2008. A late Pleistocene long pollen record from Lake Urmia, NW Iran. Quat. Res. 69, 413–420. https://doi.org/10.1016/j.yqres.2008.03.004.
Djamali, M., de Beaulieu, J.-L., Andrieu-Ponel, V., Berberian, M., Miller, N.F., Gandouin, E., Lahijani, H., Shah-Hosseini, M., Ponel, P., Salimian, M., Guitera, F., 2009. A late Holocene pollen record from Lake Almalou in NW Iran: evidence for changing land-use in relation to some historical events during the last 3700 years. J. Archaeol. Sci. 36, 1364–1375. https://doi.org/10.1016/j.jas.2009.01.022.
Dray, S., Dufour, A.-B., 2007. The ade4 package: implementing the duality diagram for ecologists. J. Stat. Software 22, 1–20.
Dugerdil, L., Joannin, S., Peyron, O., Jouffroy-Bapicot, I., Vannière, B., Boldgiv, B., Ménot, G., in review, 2020. Climate reconstructions based on GDGTs and pollen surface datasets from Mongolia and Siberia: calibrations and applicability to extremely dry and cold environments. Biogeosci. Discuss. https://doi.org/10.5194/bg-2019-475.
El-Moslimany, A.P., 1990. Ecological significance of common nonarboreal pollen: examples from drylands of the Middle East. Rev. Palaeobot. Palynol. 64, 343–350.
Faegri, K, Iversen, J, 1989. Textbook of Pollen Analysis (revised by Fægri, K., Kaland, P.E. and Krzywinski, K.)., IV. Wiley and Sons, Chichester.
Fayvush, G., Aleksanyan, A., Bussmann, R.W., 2017. Ethnobotany of the Caucasus – Armenia. In: Bussmann, R.W. (Ed.), Ethnobotany of the Caucasus. Springer, Cham, pp. 21–36. https://doi.org/10.1007/978-3-319-49412-8_18.
Fick, S.E., Hijmans, R.J., 2017. WorldClim 2: new 1-km spatial resolution climate surfaces for global land areas. Int. J. Climatol. 37, 4302–4315.
Franklin, K.J., 2014a. "This World Is an Inn:" Cosmopolitanism and Caravan Trade in Late Medieval Armenia. Doctoral Dissertation. The University of Chicago.
Franklin, K.J., 2014b. A house for trade, a space for politics: excavations at the Arai-Bazarjugh Late Medieval Caravanatun, Armenia. Anatolica 40, 1–21.
Gasparyan, B., Adler, D.S., Egeland, C.P., Azatyan, K., 2014. Recently discovered lower paleolithic sites of Armenia. In: Gasparyan, B., Arimura, M. (Eds.), Stone Age of Armenia: A Guide-Book to the Stone Age Archaeology in the Republic of Armenia. Center for Cultural Resource Studies, Kanazawa University, Kanazawa, pp. 37–64.
Gevorgyan, H., Breitkreuz, C., Meliksetian, K., Israyelyan, A., Ghukasyan, Y., Pfänder, J., Sperner, B., Miggins, D., Koppers, A., 2020. Quaternary ring plain- and valley-confined pyroclastic deposits of Aragats stratovolcano (Lesser Caucasus): Lithofacies, geochronology and eruption history. Journal of Volcanology and Geothermal Research 401, 1–20. https://doi.org/10.1016/j.jvolgeores.2020.106928.
Greene, A.F., 2013. The Social Lives of Pottery on the Plain of Flowers: an Archaeology of Pottery Production, Distribution, and Consumption in the Late Bronze Age South Caucasus. Ph.D. thesis. The University of Chicago.
Guiot, J., 1990. Methodology of the last climatic cycle reconstruction in France from pollen data. Palaeogeogr. Palaeoclimatol. Palaeoecol. 80, 49–69. https://doi.org/10.1016/0031-0182(90)90033-4.
Heiri, O., Lotter, A.F., Lemcke, G., 2001. Loss on ignition as a method for estimating organic and carbonate content in sediments: reproducibility and comparability of results. J. Paleolimnol. 25, 101–110. https://doi.org/10.1023/A:1008119611481.
Higuera, P.E., Peters, M.E., Brubaker, L.B., Gavin, D.G., 2007. Understanding the origin and analysis of sediment-charcoal records with a simulation model. Quat. Sci. Rev. 26, 1790–1809. https://doi.org/10.1016/j.quascirev.2007.03.010.
Higuera, P.E., Brubaker, L.B., Anderson, P.M., Hu, F.S., Brown, T.A., 2009. Vegetation mediated the impacts of postglacial climate change on fire regimes in the south-central Brooks Range, Alaska. Ecol. Monograph 79, 201–219. https://doi.org/10.1890/07-2019.1.
Hovsepyan, R., 2008. Appendix 2: the palaeobotanical remains from early Bronze age Gegharot. In: Badalyan, R., Smith, A., Lindsay, I., Khatchadourian, L., Avetisyan, P. (Eds.), Village, fortress, and town in Bronze and Iron Age Southern Caucasia: A preliminary report on the 2003–2006 investigations of Project ArAGATS on the Tsaghkahovit Plain, Republic of Armenia. Archäologische Mitteilungen aus Iran und Turan, vol. 40, pp. 90–96.
Hovsepyan, R., 2014. Appendix 1: archaeobotanical investigations at Iron III Tsaghkahovit. In: Khatchadourian, L. (Ed.), Empire in the Everyday: A Preliminary Report on the 2008–2011 Excavations at Tsaghkahovit, Armenia. Am. J. Archaeol, vol. 118, p. 163. https://doi.org/10.3764/aja.118.1.0137.
Hovsepyan, R., Willcox, G., 2008. The earliest finds of cultivated plants in Armenia: evidence from charred remains and crop processing residues in pisé from the Neolithic settlements of Aratashen and Aknashen. Veg. Hist. Archaeobotany 17, S63–S71. https://doi.org/10.1007/s00334-008-0158-6.
Jenderedjian, K., 2005. Peatlands of Armenia. In: Steiner, G.M. (Ed.), Moore von Sibirien bis Feuerland / Mires-from Siberia to Tierra Del Fuego. Biologiezentrum/Oberösterreichische Landesmuseen, Linz, pp. 323–333.
Joannin, S., Ali, A.A., Ollivier, V., Roiron, P., Peyron, O., Chevaux, S., Nahapetyan, S., Tozalakyan, P., Karakhanyan, A., Chataigner, C., 2014. Vegetation, fire and climate history of the Lesser Caucasus: a new Holocene record from Zarishat fen (Armenia). J. Quat. Sci. 29, 70–82. https://doi.org/10.1002/jqs.2679.
Jude, F., Marguerie, D., Badalyan, R., Smith, A.T., Delwaide, A., 2016. Wood resource management based on charcoals from the Bronze Age site of Gegharot (central Armenia). Quat. Int. 395, 31–44. https://doi.org/10.1016/j.quaint.2015.04.019.
Juggins, S., 2017. Rioja: Analysis of Quaternary Science Data. R package version (0.9-21). http://cran.r-project.org/package=rioja.
Kaniewski, D., Marriner, N., Cheddadi, R., Guiot, J., Van Campo, E., 2018. The 4.2 ka BP event in the Levant. Clim. Past 14, 1529–1542. https://doi.org/10.5194/cp-14-1529-2018.
Kassambara, A., Mundt, F., 2017. Factoextra: Extract and Visualize the Results of Multivariate Data Analyses, R Package Version 1.0.5. https://CRAN.R-project.org/package=factoextra.
Kelly, R.F., Higuera, P.E., Barrett, C.M., Hu, F.S., 2011. Short Paper: a signal-to-noise index to quantify the potential for peak detection in sediment-charcoal records. Quat. Res. 75, 11–17. https://doi.org/10.1016/j.yqres.2010.07.011.
Khatchadourian, L., 2008. Social Logistics under Empire: the Armenian 'Highland Satrapy' and Achaemenid Rule, Ca. 600–300 BC. PhD Thesis. University of Michigan.
Khatchadourian, L., 2014. Empire in the everyday: a preliminary report on the 2008–2011 excavations at Tsaghkahovit,. Armenia. Am. J. Archaeol 118, 137–169. https://doi.org/10.3764/aja.118.1.0137.
Legendre, P., Birks, H.J.B., 2012. From classical to canonical ordination. In: Birks, H.J.B., Lotter, A.F., Juggins, S., Smol, J.P. (Eds.), Tracking Environmental Change Using Lake Sediments, 5. Data Handling and Numerical Techniques. Springer, Dordrecht, pp. 201–248.
Leroyer, C., Joannin, S., Aoustin, D., Ali, A.A., Peyron, O., Ollivier, V., Tozalakyan, P., Karakhanyan, A., Jude, F., 2016. Mid Holocene vegetation reconstruction from Vanevan peat (south-eastern shore of Lake Sevan, Armenia). Quat. Int. 395, 5–18. https://doi.org/10.1016/j.quaint.2015.06.008.
Leys, B., Brewer, S.C., McConaghy, S., Mueller, J., McLauchlan, K.K., 2015. Fire history reconstruction in grassland ecosystems: amount of charcoal reflects local area burned. Environ. Res. Lett. 10, 1–14.
Leys, B., Higuera, P.E., McLauchlan, K.K., Dunnette, P.V., 2016. Wildfires and geochemical change in a subalpine forest over the past six millennia. Environ.

Res. Lett. 11, 125003.
Leys, B.A., Commerford, J.L., McLauchlan, K.K, 2017. Reconstructing grassland fire history using sedimentary charcoal: Considering count, size and shape. PLOS One 12 (4), 1–15. https://doi.org/10.1371/journal.pone.0176445.
Lindsay, I., 2006. Late Bronze Age Power Dynamics in Southern Caucasia: A Community Perspective on Political Landscapes. PhD Thesis. University of California, Santa Barbara.
Litt, T., Krastel, S., Sturm, M., Kipfer, R., Örcen, S., Heumann, G., Franz, S.O., Ülgen, U.B., Niessen, F., 2009. 'PALEOVAN', international continental scientific drilling program (ICDP): site survey results and perspectives. Quat. Sci. Rev. 28, 1555–1567. https://doi.org/10.1016/j.quascirev.2009.03.002.
Lydolph, P.E., 1977. Climates of the Soviet Union, World Survey of Climatology, 7. Elsevier, Amsterdam.
Manning, S.W., Smith, A.T., Khatchadourian, L., Badalyan, R., Lindsay, I., Greene, A., Marshall, M., 2018. A new chronological model for the Bronze and Iron age South Caucasus: radiocarbon results from Project ArAGATS, Armenia. Antiquity 92, 1530–1551. https://doi.org/10.15184/aqy.2018.171.
Marshall, M.E., 2014. Subject(ed) Bodies: A Bioarchaeological Investigation of Late Bronze Age–Iron I (1500–800 BC), Armenia. Doctoral Dissertation. University of Chicago.
McPherson, G.R., 1995. The role of fire in the desert grasslands. In: McClaran, M., Van Devender, T.R. (Eds.), The Desert Grassland. University of Arizona Press, Tucson, pp. 130–151.
Merola-Zwartjes, M., 2004. Biodiversity, functional processes, and the ecological consequences of fragmentation in southwestern grasslands. In: Finch, Deborah M. (Ed.), 2004. Assess. Grassl. Ecosyst. Cond. Southwest. United States, vol. 1. CO US Dep. Agric. For. Serv. Rocky Mt. Res. Sta 1, Fort Collins. Gen. Tech. Rep. RMRS-GTR-135-vol. 1.
Messager, E., Belmecheri, S., Von Grafenstein, U., Nomade, S., Ollivier, V., Voinchet, P., Puaud, S., Courtin-Nomade, A., Guillou, H., Mgeladze, A., Dumoulin, J.-P., Mazuy, A., Lordkipanidze, D., 2013. Late Quaternary record of the vegetation and catchment-related changes from Lake Paravani (Javakheti, South Caucasus). Quat. Sci. Rev. 77, 125–140. https://doi.org/10.1016/j.quascirev.2013.07.011.
Messager, E., Nomade, S., Wilhelm, B., Joannin, S., Scao, V., Von Grafenstein, U., Martkoplishvili, I., Ollivier, V., Mgeladze, A., Dumoulin, J.-P., Mazuy, A., Belmecheri, S., Lordkipanidze, D., 2017. New pollen evidence from Nariani (Georgia) for delayed postglacial forest expansion in the South Caucasus. Quat. Res. 87, 121–132. https://doi.org/10.1017/qua.2016.3.
Mitchell, J., Westaway, R., 1999. Chronology of Neogene and Quaternary uplift and magmatism in the Caucasus: constraints from K–Ar dating of volcanism in Armenia. Tectonophysics 304, 157–186. https://doi.org/10.1016/S0040-1951(99)00027-X.
Monahan, B., 2008. Appendix 1: the faunal remains. In: Badalyan, R., Smith, A., Lindsay, I., Khatchadourian, L., Avetisyan, P. (Eds.), Village, fortress, and town in Bronze and Iron Age Southern Caucasia: A preliminary report on the 2003–2006 investigations of Project ArAGATS on the Tsaghkahovit Plain, Republic of Armenia. Archäologische Mitteilungen aus Iran und Turan, vol. 40, pp. 90–96.
Monahan, B., 2014. Appendix 2: zooarchaeological investigations at Iron III Tsaghkahovit. In: Khatchadourian, L. (Ed.), Empire in the Everyday: A Preliminary Report on the 2008–2011 Excavations at Tsaghkahovit, Armenia. Am. J. Archaeol, vol. 118, pp. 163–166. https://doi.org/10.3764/aja.118.1.0137.
Montoya, C., Balasescu, A., Joannin, S., Ollivier, V., Liagre, J., Nahapetyan, S., Ghukasyan, R., Colonge, D., Gasparyan, B., Chataigner, C., 2013. The Upper Palaeolithic site of Kalavan 1 (Armenia): an Epigravettian settlement in the Lesser Caucasus. J. Hum. Evol. 65, 621–640. https://doi.org/10.1016/j.jhevol.2013.07.011.
Moore, P., Webb, J.A., Collinson, M.E., 1991. Pollen Analysis. Blackwell Scientific Publications, London.
Mulkidzhanian, IA.I., 1975. K istorii arboriflory Armianskoĭ SSR (On the history of arboriflora in Armenian SSR). Flora, Rastit. i Rastit. Resur. Armianskoĭ SSR (Flora, Veg. plant Resour. Armen. SSR) 6, 120–146 (In Russian).
Nakhutsrishvili, G., 2013. The Vegetation of Georgia (South Caucasus). Springer-Verlag, Heidelberg. https://doi.org/10.1007/978-3-642-29915-5.
Nalivkin, D.V., 1973. Geology of the USSR. University of Toronto Press, Toronto.
Nestler, A., Huss, M., Ambartzumian, R., Hambarian, A., 2014. Hydrological implications of covering wind-blown snow accumulations with geotextiles on Mount Aragats, Armenia. Geosciences 4, 73–92. https://doi.org/10.3390/geosciences4030073.
Oksanen, J., Blanchet, F.G., Friendly, M., Kindt, R., Legendre, P., McGlinn, D., Minchin, P.R., O'Hara, R.B., Simpson, G.L., Solymos, P., Stevens, M.H.H., Szoecs, E., Wagner, H., 2019. Vegan: community ecology package. R package version 2.5-6. https://CRAN.R-project.org/package=vegan.
Peyron, O., Guiot, J., Cheddadi, R., Tarasov, P., Reille, M., de Beaulieu, J.-L., Bottema, S., Andrieu, V., 1998. Climatic reconstruction in Europe for 18,000 YR B.P. from pollen data. Quat. Res. 49, 183–196. https://doi.org/10.1006/qres.1997.1961.
Prentice, I.C., Guiot, J., Huntley, B., Jolly, D., Cheddadi, R., 1996. Reconstructing biomes from palaeoecological data: a general method and its application to European pollen data at 0 and 6 ka. Clim. Dynam. 12, 185–194.
Quantum, G.I.S., Development Team, 2016. QGIS Geographic Information System. Open Source Geospatial Foundation Project.
R Development Core Team, 2017. R: A Language and Environment for Statistical Computing. R Found. Stat. Comput, Vienna, Austria. http://www.R-project.org/.
Reille, M., 1992-1998. Pollen et Spores d'Europe et d'Afrique du nord, Laboratoire de Botanique Historique et Palynologie. Universite d'Aix-Marseille, Marseille.
Reimer, P.J., Bard, E., Bayliss, A., Beck, J.W., Blackwell, P.G., Ramsey, C.B., Buck, C.E., Cheng, H., Edwards, R.L., Friedrich, M., Grootes, P.M., Guilderson, T.P., Halfidason, H., Hajdas, I., Hatté, C., Heaton, T.J., Hoffmann, D.L., Hogg, A.G., Hughen, K.A., Kiaser, K.F., Kromer, B., Manning, S.W., Niu, M., Reimer, R.W., Richards, D.A., Scott, E.M., Southon, J.R., Staff, R.A., Turney, C.S.M., van der Plicht, J., 2013. IntCal13 and Marine13 radiocarbon age calibration curves 0–50,000 years cal BP. Radiocarbon 55, 1869–1887. https://doi.org/10.2458/azu_js_rc.55.16947.
Richter, T.O., van der Gaast, S., Koster, B., Vaars, A., Gieles, R., de Stigter, H.C., De Haas, H., van Weering, T.C.E., 2006. The Avaatech XRF Core Scanner: technical description and applications to NE Atlantic sediments. Geol. Soc. London,. Spec. Publ. 267, 39–50. https://doi.org/10.1144/GSL.SP.2006.267.01.03.
Roberts, N., 2002. Did prehistoric landscape management retard the post-glacial spread of woodland in Southwest Asia? Antiquity 76, 1002–1010. https://doi.org/10.1017/S0003598X0009181X.
Roberts, N., Eastwood, W.J., Kuzucuoğlu, C., Fiorentino, G., Caracuta, V., 2011. Climatic, vegetation and cultural change in the eastern Mediterranean during the mid-Holocene environmental transition. The Holocene 21, 147–162. https://doi.org/10.1177/0959683610386819.
Rossignol-Strick, M., 1995. Sea-land correlation of pollen records in the Eastern Mediterranean for the glacial-interglacial transition: biostratigraphy versus radiometric time-scale. Quat. Sci. Rev. 14, 893–915. https://doi.org/10.1016/0277-3791(95)00070-4.
Sabatier, P., Dezileau, L., Briqueu, L., Colin, C., Siani, G., 2010. Clay minerals and geochemistry record from northwest Mediterranean coastal lagoon sequence: implications for paleostorm reconstruction. Sediment. Geol. 228, 205–217. https://doi.org/10.1016/j.sedgeo.2010.04.012.
Sabatier, P., Wilhelm, B., Ficetola, G.F., Moiroux, F., Poulenard, J., Develle, A.-L., Bichet, A., Chen, W., Pignol, C., Reyss, J.-L., Ludovic, G., Bajard, M., Perrette, Y., Malet, E., Taberlet, P., Arnaud, F., 2017. 6-kyr record of flood frequency and intensity in the western Mediterranean Alps - interplay of solar and temperature forcing. Quat. Sci. Rev. 170, 121–135. https://doi.org/10.1016/j.quascirev.2017.06.019.
Sagona, A., 2017. The archaeology of the Caucasus: from earliest settlements to the Iron Age, Cambridge World Archaeology. In: Cambridge University Press, Cambridge.
Sharifi, A., Pourmand, A., Canuel, E.A., Ferer-Tyler, E., Peterson, L.C., Aichner, B., Feakins, S.J., Daryaee, T., Djamali, M., Beni, A.N., Lahijani, H.A.K., Swart, P.K., 2015. Abrupt climate variability since the last deglaciation based on a high-resolution, multi-proxy peat record from NW Iran: the hand that rocked the Cradle of Civilization? Quat. Sci. Rev. 123, 215–230. https://doi.org/10.1016/j.quascirev.2015.07.006.
Shumilovskikh, L.S., Tarasov, P., Arz, H.W., Fleitmann, D., Marret, F., Nowaczyk, N., Plessen, B., Schlütz, F., Behling, H., 2012. Vegetation and environmental dynamics in the southern Black Sea region since 18 kyr BP derived from the marine core 22-GC3. Palaeogeogr. Palaeoclimatol. Palaeoecol. 337–338, 177–193. https://doi.org/10.1016/j.palaeo.2012.04.015.
Smith, A.T., 2015. The Political Machine: Assembling Sovereignty in the Bronze Age Caucasus. Princeton University Press, Princeton.
Smith, A.T., Badalyan, R.S., Avetisyan, P., Greene, A., Minc, L., 2009. The Archaeology and Geography of Ancient Transcaucasian Societies, Volume 1: The Foundations of Research and Regional Survey in the Tsaghkahovit Plain, Armenia, I. Oriental Institute Publications, Chicago.
Smith, A.T., Leon, J.F., 2014. Divination and sovereignty: the Late Bronze Age shrines at Gegharot, Armenia. Am. J. Archaeol. 118, 549–563. https://doi.org/10.3764/aja.118.4.0549.
Solomon, J.C., Shulkina, T.V., Schatz, G.E., 2014. Red List of the Endemic Plants of the Caucasus: Armenia, Azerbaijan, Georgia, Iran, Russia, and Turkey. Missouri Botanical Garden Press, Saint Louis.
Staubwasser, M., Weiss, H., 2006. Holocene climate and cultural evolution in late prehistoric–early historic west Asia. Quat. Res. 66, 372–387. https://doi.org/10.1016/j.yqres.2006.09.001.
Takhtajan, A., 1941. Botanico-geographicheskij ocherk armenii [Phyto-geographical review of Armenia]. Proc. Inst. Bot. Armen. branch USSR Acad. Sci. 2, 3–156.
Tarasov, P.E., Cheddadi, R., Guiot, J., Bottema, S., Peyron, O., Belmonte, J., Ruiz-Sanchez, V., Saadi, F., Brewer, S., 1998. A method to determine warm and cool steppe biomes from pollen data; application to the Mediterranean and Kazakhstan regions. J. Quat. Sci. 13, 335–344. https://doi.org/10.1002/(SICI)1099-1417(199807/08)13:4<335::AID-JQS375>3.0.CO;2-A.
Turner, R., Roberts, N., Jones, M.D., 2008. Climatic pacing of Mediterranean fire histories from lake sedimentary microcharcoal. Global Planet. Change 63, 317–324. https://doi.org/10.1016/j.gloplacha.2008.07.002.
Turner, R., Roberts, N., Eastwood, W.J., Jenkins, E., Rosen, A., 2010. Fire, climate and the origins of agriculture: micro-charcoal records of biomass burning during the last glacial–interglacial transition in Southwest Asia. J. Quat. Sci. 25, 371–386. https://doi.org/10.1002/jqs.1332.
Van Geel, B., 2002. Non-pollen palynomorphs. In: Smol, J.P., Birks, H.J.B., Last, W.M., Bradley, R.S., Alverson, K. (Eds.), Tracking Environmental Change Using Lake Sediments, vol. 3. Terrestrial, algal, and silicaceous indicators. Springer, Dordrecht, pp. 99–109. https://doi.org/10.1007/0-306-47668-1_6.
Van Zeist, W., Bottema, S., 1977. Palynological investigations in western Iran. Palaeohistoria 19, 19–85.
Van Zeist, W., Woldring, H., Stapert, D., 1975. Late Quaternary vegetation and climate of southwestern Turkey. Palaeohistoria 17, 53–143.

Volodicheva, N., 2002. The Caucasus. In: Shahgedanova, M. (Ed.), The Physical Geography of Northern Eurasia. Oxford University Press, New York, pp. 350–376.
Vysotsky, G.N., 1905. Stepi evropeiskoi rossii (steppes of European Russia). In: Filipuyev, V.I. (Ed.), Polnaya Entsiklopediya Russkogo Selskogo Hozyaistva. The Complete Encyclopedia of Russian Agriculture, St. Petersburg, pp. 397–443 (In Russian).
Walker, M.J.C., Berkelhammer, M., Björck, S., Cwynar, L.C., Fisher, D.A., Long, A.J., Lowe, J.J., Newnham, R.M., Rasmussen, S.O., Weiss, H., 2012. Formal subdivision of the Holocene series/epoch: a discussion paper by a working group of INTIMATE (integration of ice-core, marine and terrestrial records) and the subcommission on quaternary stratigraphy (international commission on stratigraphy). J. Quat. Sci. 27, 649–659. https://doi.org/10.1002/jqs.2565.
Wesche, K., Treiber, J., 2012. Abiotic and biotic determinants of steppe productivity and performance - a View from central Asia. In: Werger, M.J.A., van Staalduien, M.A. (Eds.), Eurasian Steppes. Ecological Problems and Livelihoods in a Changing World. Springer, Dordrecht, pp. 3–43.
Whitlock, C., Larsen, C., 2002. Charcoal as a fire proxy. In: Smol, J.P., Birks, H.J.B., Last, W.M., Bradley, R.S., Alverson, K. (Eds.), Tracking Environmental Change Using Lake Sediments, vol. 3. Terrestrial, Algal, and Siliceous Indicators. Springer, Dordrecht, pp. 75–97.
Wick, L., Lemcke, G., Sturm, M., 2003. Evidence of Lateglacial and Holocene climatic change and human impact in eastern Anatolia: high-resolution pollen, charcoal, isotopic and geochemical records from the laminated sediments of Lake Van, Turkey. The Holocene 13, 665–675.
Woodbridge, J., Roberts, C.N., Palmisano, A., Bevan, A., Shennan, S., Fyfe, R., Eastwood, W.J., Izdebski, A., Çakirlar, C., Woldring, H., Broothaerts, N., Kaniewski, D., Finné, M., Labuhn, I., 2019. Pollen-inferred regional vegetation patterns and demographic change in Southern Anatolia through the Holocene. The Holocene 29, 728–741. https://doi.org/10.1177/0959683619826635.
Wright, H.E.J., Ammann, B., Stefanova, I., Atanassova, J., Margalitadze, N., Wick, L., Blyakharchuk, T., 2003. Late-glacial and early-holocene dry climates from the balkan peninsula to southern siberia. In: Tonkov, S. (Ed.), Aspects of Palynology and Palaeoecology. Festschrift in Honour of Elissaveta Bozilova. Pensoft Publishers., Sofia, pp. 127–136.
Zibtsev, S., Mitsopoulos, I., Mallinis, G., Saglam, B., Borsuk, A., Zaimes, N., Yavuz, M., Galupa, D., Emmanouloudis, D., Uratu, R., Moisei, R., Ghulijanyan, A., 2014. Wild land fires in the black sea region: impact, management and needs for innovative technologies. Int. Sci. Electron. J. Earth Bioresour. Life Qual. Founded by Natl. Univ. Life Environ. Sci. Ukr. (NUBiP Ukr. Glob. Consort. High. Educ. Res. Agric.) 4.